

# **Ionic Liquids for Application in Separation Processes: Chromatographic and Calorimetric Studies**

**Sabrina Barbosa Rosini**

Dissertation presented to

**Escola Superior de Tecnologia e Gestão  
Instituto Politécnico de Bragança**

In order to obtain Master's Degree in

**Chemical Engineering**

This work was supervised by

**Simão Pedro Pinho**

**Maria Olga Ferreira**

**Priscilla Leite**

Bragança  
March, 2020

**“Who am I, Lord, to remember me?  
To bring me here, and make me such beautiful things?”**

Mike Michele Kunert Deps

## Acknowledgments

I am grateful for this moment in my life. I have never imagined that one day, I will be capable to study and conquest the title of Master's degree in Chemical Engineering. Of course, if I had not had the help of wonderful people to stay of by my side, I never would have made it.

So, I want to thank God that who never let me feel alone in a totally unknown place. I also express my gratitude to my supervisors from IPB, professors Simão Pinho and Olga Ferreira, together you are a perfect pair of mentors, the professor Olga that always help me to structure the path of the execution of my research, and professor Simão, that even without realizing it motivated me to develop a good work, in our meetings. Thank you for understanding my confused routine.

I cannot let to thank professors Priscila Leite, Juliana Peitrobelli, and Erica Lovo for offering me and incentive me to attend the Double Degree Program formed by the partnership of UTFPR and IPB.

I also thank to my family that give me all emotionally and more important support. My parents Otávio Rosini and Iliane Rosini that neve measured efforts to I have a good education, and always gave me love. My brothers Bárbara Rosini and Jonathan Rosini, you showed me that the distance is nothing if we compare with how I am missing you. And I am immensely grateful to my husband Elimar that always help me, give me supports, was my best friend and encouragement me during this whole process. Without you I wouldn't be able to conclude this work.

My special thanks to Sérgio that always when I asked for help, he was promptly willing to resolve my doubts, and how many times he and Gabriel helped me with the equipment. Without you, surely my work would not have the same result.

I also thank to people of laboratory LSRE who contributed to make this experience lighter and always with humor and joy. And of course, thank to Laboratory of Separation and Reaction Engineering (LSRE) for providing me all the facilities and equipment to reach the outcomes of this work.

This work would not have been the same without the contribution of all the people mentioned above, and of course, my friends who have always supported me. I wouldn't be the same without you, so thank you so much.

## Abstract

The family of ionic liquids can provide safer, efficient and more sustainable alternative solvents than those commonly used. In this work, 1-butyl-3-methylimidazolium acetate (BmimAc) was the selected ionic liquid to be studied as a separation agent in different liquid-liquid extraction problems with terpenes and terpenoids. After separation, it is important to devise a strategy to recover the IL and minimize costs.

To do so, infinite dilution activity coefficients of water and 44 solutes belonging to different families of organic compounds, were measured in the ionic liquid by gas chromatography. This ionic liquid showed strong interaction with polar solutes like alcohols and linalool, for which low values of activity coefficients at infinite dilution were obtained. Concerning the system limonene/linalool (compounds used in biodegradable solvents and perfumery industries), this IL showed the best values of capacity and selectivity, calculated through activity coefficients. However, it was not a good separation agent of the mixture  $\alpha$ -pinene/ $\beta$ -pinene (used in used in medications with antifungal action).

Besides that, the solid-liquid equilibria phase diagram was studied by differential scanning calorimetry (DSC), by measuring the freezing point depression of water caused by the addition of 1-butyl-3-methylimidazolium acetate. The methodology was tested first by measuring the freezing point of aqueous solutions of NaCl, CaCl<sub>2</sub>, 2-propanediol and 1-ethyl-3-methylimidazolium acetate (EmimAc). The values obtained in this work agreed with literature, except for the 1-ethyl-3-methylimidazolium acetate. So, further tests need to be carried out using other methodologies. Through the measurement of freezing point curves, important data were obtained concerning the 1-butyl-3-methylimidazolium acetate (BmimAc)+ water interactions. Thus, crystallization is a possible process for separating ILs from water.

This work offers a solution to separate the system limonene/linalool and then recovery the IL through freezing point depression of water/BmimAc once that was possible freeze the water.

**Keywords:** ionic liquid, infinite dilution activity coefficients, gas chromatography, freezing point depression, differential scanning calorimetry

## Resumo

A família de líquidos iônicos pode fornecer solventes alternativos mais seguros, eficientes e mais sustentáveis do que os comumente usados. Neste trabalho, acetato de 1-butil-3-metilimidazólio (BmimAc) foi o líquido iônico selecionado para ser estudado como um agente de separação em diferentes problemas de extração líquido-líquido com terpenos e terpenóides. Após a separação, é importante conceber uma estratégia para recuperar o LI e minimizar os custos.

Para isso, foram medidos coeficientes de atividade a diluição infinita de água e 44 solutos pertencentes a diferentes famílias de compostos orgânicos, no líquido iônico, por cromatografia gasosa. Este líquido iônico mostrou forte interação com solutos polares como álcoois e linalol, para os quais foram obtidos baixos valores de coeficientes de atividade em diluição infinita. No que diz respeito ao sistema limoneno / linalol (compostos utilizados como solventes biodegradáveis e na indústria de perfumaria), este IL mostrou os melhores valores de capacidade e seletividade. No entanto, não foi um bom agente de separação da mistura  $\alpha$ -pineno /  $\beta$ -pineno (usados em medicamentos com ação anti-fúngica).

Além disso, o diagrama de fases de equilíbrio sólido-líquido foi estudado por calorimetria diferencial de varredura (DSC), medindo a depressão do ponto de congelamento da água causada pela adição de acetato de 1-butil-3-metilimidazólio. A metodologia foi testada primeiro medindo o ponto de congelamento de soluções aquosas de NaCl, CaCl<sub>2</sub>, 2-propanodiol e acetato de 1-etil-3-metilimidazólio (EmimAc). Os valores obtidos neste trabalho concordam com a literatura, exceto o acetato de 1-etil-3-metilimidazólio. Portanto, testes adicionais precisam ser realizados usando outras metodologias.

Através da medição das curvas do ponto de congelamento, foram obtidos dados importantes sobre as interações 1-butil-3-metilimidazólio + água. Assim, a cristalização é um processo possível para separar ILs da água.

Este trabalho oferece uma solução para a separação do sistema limoneno/linalol e a recuperação do LI usado no sistema por meio do abaixamento do ponto de congelamento da água em contato com o BmimAc, uma vez que foi possível cristalizar a água da mistura.

**Palavras-chave:** líquido iônico, coeficientes de atividade a diluição infinita, cromatografia gasosa, abaixamento do ponto de fusão, calorimetria diferencial de varredura



## Table of Contents

|  |    |
|--|----|
| Chapter 1. Main goals and context of this work.....                  | 1  |
| Chapter 2. Introduction.....   | 3  |
| 2.1. Ionic liquids.....  | 3  |
| 2.2. Activity coefficients measurements by gas chromatography.....   | 6  |
| 2.2.1. Methodology.....  | 7  |
| 2.2.2. Theoretical principles.....                                   | 9  |
| 2.3. Freezing point measurements.....                                | 10 |
| 2.3.1. Methodology I - Beckmann apparatus.....                       | 13 |
| 2.3.2. Methodology II – Heriot-Watt University apparatus.....        | 15 |
| 2.3.3. Methodology III - Differential scanning calorimetry.....      | 16 |
| Chapter 3. Experimental infinite dilution activity coefficients..... | 18 |
| 3.1. Chemicals.....  | 18 |
| 3.2. Experimental methodology selected in this work.....             | 22 |
| 3.3. Experimental activity coefficient at infinite dilution.....     | 23 |
| Chapter 4. Experimental freezing point depression.....               | 31 |
| 4.1. Chemicals.....  | 31 |
| 4.2. Experimental methodology.....                                   | 32 |
| 4.3. Aqueous solutions of NaCl.....                                  | 37 |
| 4.4. Aqueous solutions of CaCl <sub>2</sub> .....                    | 38 |
| 4.5. Aqueous solutions of 1,2-propanediol.....                       | 40 |
| 4.6. Aqueous solutions of 1-ethyl-3-methylimidazolium acetate.....   | 42 |
| 4.7. Aqueous solutions of 1-butyl-3-methylimidazolium acetate.....   | 45 |
| Chapter 5. Conclusions and future work.....                          | 49 |
| References.....  | 51 |
| Appendix A.....  | 55 |
| Appendix B.....  | 62 |

## List of Symbols and Acronyms

|  |   |
|--|---|
| AcIL                                     | Ionic liquid with acetate as anion                                |
| BmimAc                                   | 1-butyl-3-methylimidazolium acetate                               |
| $B_{11}$                                 | Second virial coefficient of the pure solute                      |
| $B_{12}$                                 | Cross second virial coefficient of the solute and the carrier gas |
| $C_{\text{alkyl}}$                       | Carbon alkyl chain  |
| CAS                                      | Chemical Abstracts Number   |
| $C_{\text{ring}}$                        | Ring carbon   |
| $\Delta C_p$                             | Heat capacity   |
| DSC                                      | Differential scanning calorimetry                                 |
| DTA                                      | Differential thermal analysis                                     |
| EmimAc                                   | 1-ethyl-3-methylimidazolium acetate                               |
| $f_1^L$                                  | Fugacity of the pure compound 1                                   |
| $f_1^S$                                  | Fugacity of compound 1 in a solid phase                           |
| $\bar{G}_m^{E,\infty}$                   | Partial molar excess of Gibbs free energy                         |
| GLC                                      | Gas-liquid chromatography   |
| $\bar{H}_m^{E,\infty}$                   | Partial molar excess enthalpy                                     |
| $\Delta \underline{H}^{\text{fus}}(T_m)$ | Heat of fusion at normal melting point temperature                |
| IL                                       | Ionic liquid  |



|                        |   |
|------------------------|---|
| $J_2^3$                | Term of pressure correction                 |
| $k_j^\infty$           | Capacity                                    |
| $K_L$                  | Gas-liquid partition coefficient            |
| $m_3$                  | Mass of ionic liquid                        |
| NMR                    | Nuclear Magnetic Resonance                  |
| $n_3$                  | Number of moles of solvent                  |
| PTFE                   | Poly(tetrafluoroethylene)                   |
| $P_0$                  | Outlet pressure                             |
| $P_1^*$                | Saturated vapor pressure                    |
| $P_i$                  | Inlet pressure                              |
| R                      | Gas constant                                |
| $S_{ij}^\infty$        | Selectivity between the solutes $i$ and $j$ |
| $\bar{S}_m^{E,\infty}$ | Partial molar excess entropy                |
| SLE                    | Solid-liquid equilibria                     |
| $t_G$                  | Retention time of air                       |
| $t_R$                  | Retention time of solute                    |
| TBP                    | Boiling point temperature                   |
| TCD                    | Thermal conductivity detector               |
| $T_f$                  | Deviation from the baseline due to fusion   |
| $T_f$                  | Temperature of freeze of solvent            |

|                      |  |
|----------------------|--|
| TGA                  | Thermogravimetric analysis   |
| $T_i$                | First deviation from the baseline  |
| $T_m$                | Melting point  |
| $\Delta T$           | Freezing point depression  |
| $T$                  | Column temperature   |
| $U_0$                | Column outlet volumetric flow rate                                       |
| $V_1^*$              | Molar volume of the solute   |
| $V_1^\infty$         | Partial molar volume of the solute (1) at infinite dilution              |
| $V_N$                | Net retention volume   |
| $x_1$                | Mole fraction of component 1   |
| $x_2$                | Mole fraction of component 2   |
| $\gamma_{13}^\infty$ | Activity coefficients at infinite dilution of component 1 in component 3 |
| $\rho_3$             | Density of ionic liquid  |



## List of Figures

|  |    |
|--|----|
| <b>Figure 1.</b> Relative percent deviations obtained for the representation of freezing point depression for non-electrolyte and electrolyte solutions (Pinho and Macedo, 2004).....  | 12 |
| <b>Figure 2.</b> Illustration of the Beckmann equipment used by Liu et al. (2017) and Arshad et al. (2013) to measure the freezing point depression (adapted from Liu et al. (2017)): A, thermostatic bath; B, cooling jacket; C, sample glass with magnetic stirrer; D, rubber stopper with sample glass lid; E, device for manual stirring; F, ethanol bath for control temperature with magnetic stirrer; G, Pt100 thermometer; H, data acquisition unit..... | 13 |
| <b>Figure 3.</b> Temperature profile in a freezing point measurement. Adapted from Fosbøl et al. (2011).....   | 15 |
| <b>Figure 4.</b> Schematic illustration of a freezing point apparatus (Haghighi et al., 2008): A, PTFE - poly(tetrafluoroethylene) sealing sleeve; B, Sample PRT; C, Packed, saturated sample; E, Reference PRT and D, PRT sensitive region.....   | 16 |
| <b>Figure 5.</b> Chemical structure of 1-butyl-3methylimidazolium acetate BmimAc.....  | 22 |
| <b>Figure 6.</b> GC used in this work. ....  | 22 |
| <b>Figure 7.</b> Activity coefficients at infinite dilution of several solutes in 1-butyl-3-methylimidazolium acetate, at T= 403.15 K represented by $\gamma_{\infty}$ for alcohols, terpenes and terpenoids, and T= 373.15 K for the other organic compounds represented by $\gamma_{\infty}^*$ .....   | 24 |
| <b>Figure 8.</b> Activity coefficients at infinite dilution of alkanes. ....   | 24 |
| <b>Figure 9.</b> Comparison between results obtained in this work with values measured by Stark et al. (2012).....   | 25 |
| <b>Figure 10.</b> Partial molar excess properties as a function of the activity coefficients at infinite dilution of the organic solutes at 383.15 K. The line represents $G_m E_{\infty}$ and the symbols correspond to: $H_m E_{\infty}$ and $T_{ref} S_m E_{\infty}$ .....  | 26 |

|  |    |
|--|----|
| <b>Figure 11.</b> Partial molar excess energies as a function of enthalpy of the organic solutes at 383.15 K and 353.15 K. The line represents linear ( $H_{mE. \infty}$ vs $T_{ref}S_{mE. \infty}$ ). The $G_{mE. \infty}$ vs $H_{mE. \infty}$ and the symbol $\Delta$ correspond $H_{mE. \infty}$ vs $T_{ref}S_{mE. \infty}$ ..... | 27 |
| <b>Figure 12.</b> Experimental (gas + liquid) partition coefficients, $K_L$ , for organic solutes in the ILs studied. The $\Delta$ correspond the $K_L$ values at 373.2 K and $\square$ correspond at 403.5 K.....   | 28 |
| <b>Figure 13.</b> DSC used in this work.....   | 32 |
| <b>Figure 14.</b> Thermogram of water extrapolated to 273.10 K. ....   | 33 |
| <b>Figure 15.</b> Thermogram of water with different heating rates (1, 2.5, 5 and 10 K/min). ....  | 34 |
| <b>Figure 18.</b> Thermogram of 24.73% mass fraction of $CaCl_2$ . ....  | 36 |
| <b>Figure 16.</b> Freezing point depression as a function of NaCl weight percentage, comparing the results obtained in this work with literature data. ....  | 38 |
| <b>Figure 17.</b> Freezing point depression as a function of $CaCl_2$ weight percentage, comparing the results obtained in this work with literature data. ....  | 40 |
| <b>Figure 19.</b> Freezing point depression as a function of 1,2-propanediol weight fraction, comparing the results obtained in this work with literature data. ....   | 41 |
| <b>Figure 20.</b> Freezing point depression as a function of EmimAc mass fraction, comparing the results obtained in this work with literature data. ....  | 43 |
| <b>Figure 21.</b> Thermogram of 43.56% mass fraction of EmimAc. The cooling rate used was 5 K/min and the heating rates used were 1, 2.5 and 5 K/min. ....   | 44 |
| <b>Figure 22.</b> Comparison of freezing point depression for aqueous solutions of EmimAc or BmimAc.....   | 46 |
| <b>Figure 23.</b> Thermogram of 10% mass of BmimAc.....  | 47 |
| <b>Figure 24.</b> Thermogram of 10% mass of BmimAc with eutectic point. ....   | 48 |

|   |    |
|---|----|
| <b>Figure A. 1.</b> Values of activity coefficient at infinity dilution of families: alkanes and aromatics .....                    | 56 |
| <b>Figure A. 2.</b> Values of activity coefficient at infinity dilution of families: cycloalkanes and esters .....                  | 57 |
| <b>Figure A. 3.</b> Values of activity coefficient at infinity dilution of families: ethers and ketones ...                         | 58 |
| <b>Figure A. 4.</b> Values of activity coefficient at infinity dilution of families: different families and terpenes .....          | 59 |
| <b>Figure A. 5.</b> Values of activity coefficient at infinity dilution of families: butanol isomers and short-chain alcohols ..... | 60 |
| <b>Figure A. 6.</b> Values of activity coefficient at infinity dilution of families of terpenoids .....                             | 61 |
| <b>Figure A. 7.</b> Experimental (gas + liquid) partition coefficients, $K_L$ , for organic solutes.....                            | 61 |
| <b>Figure B. 1.</b> Differential scanning calorimetry of first analysis of NaCl aqueous solution.....                               | 62 |
| <b>Figure B. 2.</b> Differential scanning calorimetry of second analysis of NaCl aqueous solution ....                              | 63 |
| <b>Figure B. 3.</b> Differential scanning calorimetry of third analysis of NaCl aqueous solution.....                               | 63 |

## List of Tables

|   |    |
|---|----|
| <b>Table 1:</b> Results found in literature about the behavior of ILs for extraction and separation of terpenes. ....                                 | 8  |
| <b>Table 2.</b> Name, structure, supplier, melting point (TMP) and purity of the investigated solutes.  | 18 |
| <b>Table 3.</b> Selectivities $S^{\infty}_{ij}$ and capacities $k_j^{\infty}$ , at infinite dilution for different separation systems. ....           | 29 |
| <b>Table 4.</b> Comparison of selectivities $S^{\infty}_{ij}$ and capacities $k_j^{\infty}$ , at infinite dilution for different studies at 85°C..... | 30 |
| <b>Table 5.</b> Name, structure, supplier, melting point (TMP) and purity of the investigated solutes.  | 31 |
| <b>Table 6.</b> Freezing point data of calcium chloride aqueous solutions. ....   | 35 |
| <b>Table 7.</b> Freezing point data of 1,2-propanediol aqueous solutions.....   | 36 |
| <b>Table 8.</b> Freezing point data of sodium chloride aqueous solutions found in literature. ....  | 37 |
| <b>Table 9.</b> Freezing point data of calcium chloride aqueous solutions found in literature. ....   | 38 |
| <b>Table 10.</b> Freezing point data of 1,2-propanediol aqueous solutions found in literature.....  | 40 |
| <b>Table 11.</b> Freezing point data of EmimAc aqueous solutions.....   | 43 |
| <b>Table 12.</b> Freezing point data of BmimAc aqueous solutions. ....  | 46 |
| <b>Table A 1.</b> Values of $\gamma_{13}^{\infty}$ for all solutes. ....  | 55 |

## **Chapter 1. Main goals and context of this work**

In the last decades, the development of more environmentally friendly technologies has increased in both industry and academia being one of the objectives to eliminate or reduce the use and generation of hazardous substances (Anastas and Eghbali, 2010). In particular, the search for more sustainable, efficient and safer solvents is desirable as solvents are employed in a wide range of processes and applications involved in producing, processing, and transporting many different goods (Hayes et al., 2015). So, to find a greener substitute to the conventional volatile organic compounds (VOC), can be the solution (Huddleston et al., 1998).

Compared to VOC, ionic liquids (IL) can be tailored to present some advantages, such as low vapor pressures, low toxicity, high chemical and thermal stability, non-flammability, and are able to conduct electricity, among others. A big disadvantage, is however, their cost, so to study a way for the recovery and reuse of IL in separation processes is a crucial issue that needs to be addressed (Liu et al., 2017).

Ionic liquids result from the combination between one large organic cation and one inorganic or organic anion, with a melting point below 373 K. They are classified as designer solvents because by varying the ions, their properties can be modified and optimized for a specific objective. Thus, it is necessary to know the impact on the physical properties induced by the cation or anion, which can guarantee better and more efficient combinations, and also help to decide the best separation process for its recovery and recycling (Hayes et al., 2015; Vekariya, 2017; Wilkes, 2004).



For this reason, the number of applications of IL is increasing exponentially namely in catalysis, as solvent, as support for the immobilization of enzymes in separation technologies, as matrices for mass spectrometry, stationary phases for chromatography, supercapacitors, carbonization, lubrication, etc. (Lei et al., 2017; Zafarani-Moattar and Majdan-Cegincara, 2007).

One specific, but important application of IL, is highlighted in this work. Ionic liquids are being considered as green solvents for cellulose dissolution. In this process, water can be used in a second step as an anti-solvent for the coagulation of cellulose and to wash and remove the IL after spinning the fibers. Several recycling methods have been reported in the literature such as membrane separation, evaporation, liquid-liquid extraction, supercritical CO<sub>2</sub> extraction, centrifugal solvent-extraction, and crystallization (Liu et al., 2018; Moura Ramos and Diogo, 2009). Another application deserving our attention is the use of IL as separation agents in distillation and liquid-liquid extraction for terpenes separation and purification. These high value compounds are quite abundant in nature, having many applications in the food, perfumery, medicines and cosmetics areas (Martins et al. 2016). To understand the molecular level interactions between the IL and water, or organic compounds, is fundamental for supporting the development of extraction processes of terpenes and terpenoids using ionic liquids. To achieve that goal, the measurement of solid-liquid equilibria data or infinite dilution activity coefficients can give an important contribution, especially if complemented by molecular dynamic studies (Martins et al., 2015). Therefore, the main objectives of this work are:

- To study the solid-liquid equilibria phase diagrams of aqueous binary systems containing 1-butyl-3-methylimidazolium acetate/H<sub>2</sub>O and 1-ethyl-3-methylimidazolium acetate/H<sub>2</sub>O, by differential scanning calorimetry;

- To measure the infinite dilution activity coefficients of water and different organic solutes, namely terpenes, in ionic liquids, by gas chromatography, aiming to understand the interactions present in these complex mixtures, and to identify new entrainers to turn the separations easier.

## **Chapter 2. Introduction**

This section starts by introducing ionic liquids, and their main properties, and then the thermodynamic framework and the most common experimental measurement methods related to the activity coefficients at infinite dilution, exploring the experimental methodology and theoretical principles to comprehend the interactions between solutes and solvents.

This chapter finishes with the presentation of the topic on the freezing point of aqueous solutions are presented. Special attention was given to the DSC method, which will be applied in this work.

### **2.1. Ionic liquids**

Ionic liquids have been firstly described by Walden in 1914, when he observed organic salts that were liquid at, or close to, room temperature without additives such as water or other solvents. Ionic liquids can be briefly defined as compounds completely composed of ions with melting point below 373 K (Hermanutz et al., 2018; Lei et al., 2017). Some synonyms have been found in the literature as room temperature molten salt, liquid organic salt, ambient-temperature molten salt, low-temperature molten salt, to describe them as compounds in the liquid state at room temperature, that display ionic-covalent crystalline structures, but possible to handle like an ordinary solvent (Wasserscheid and Welton, 2002).

The number of studies about IL is increasing, indicating that more researchers are engaged in developing this area. Today, for instance, the physicochemical properties of IL are now recognized

as ranging widely from the often cited “nonvolatile, non-flammable, and air and water stable” to those that are distinctly volatile, flammable, and unstable (MacFarlane and Seddon, 2007).

Due to this, the variety of IL has grown and they have been divided into many types such as room-temperature IL (RTIL), task-specific IL (TSIL), protic liquid liquids (PIL) and supported IL membranes (SILM) that includes composites of IL supported on metal-organic frameworks (MOG) (Lei et al., 2017; Vekariya, 2017).

RTILs present fundamental features, such as strong ion-ion interaction, and are usually formed by an organic cation and an inorganic polyatomic anion, incorporating substitution group that originate a complex interplay of coulombic, hydrogen bonding, and van der Waals interactions of their ions (Wasserscheid and Welton, 2002). These substitution groups confer additional properties, either physical or chemical or in terms of reactivity as a part of the ion structure. The most popular choice for the substitution group is the alkyl substituent  $\text{CH}_3(\text{CH}_2)_n$ ; however, there are also many other choices available (Fedorov and Kornyshev, 2014; Vekariya, 2017).

Ionic liquids can show favorable physical properties such as low melting point, viscosity, density, solubility, and hydrophobicity that allow them to be easily handled. Besides that, reaction products may be separated more easily from an IL than from most of conventional solvents (Vekariya, 2017). Associating these properties with different combinations of anions and cations, the potential of ionic liquids is vast, allowing a large diversity (Crowhurst et al., 2003). These benefits make IL an attractive choice of solvent in many important chemical processes, such as in the areas of catalysis, biocatalysis, synthetic chemistry, and electrochemistry (Vekariya, 2017). However, it is not possible to identify a general set of ionic liquids properties due to the structural diversity of the ions. The only property common to IL is the ionic conductivity because they contain mobile ions with high polarity (MacFarlane and Seddon, 2007).

Besides the benefits cited previously, ILs have been studied as solvents to remove hydrocarbons from essential oils, and to separate terpenes and terpenoids (Martins et al., 2016). Terpenoids are defined as materials with molecular structures containing carbon made up of isoprene (2-methylbuta-1,3-diene) units. Isoprene contains five carbon atoms and therefore, the number of carbon atoms in any terpenoid is a multiple of five. Degradation products of terpenoids in which carbon atoms have been lost through chemical or biochemical processes may contain different numbers of carbon atoms, but their overall structure will indicate their terpenoid origin and they will still be considered as terpenoids. The terpenes are unsaturated hydrocarbons, constituted by

five carbon building block, the isoprene and they can also occur as oxygenated derivatives, called terpenoids (Martins et al., 2016). The main reason for their wide use is the abundance and diversity of these compounds in nature (Sell, 2003).

They are, however, usually present in low concentrations, so they tend to be expensive or even uneconomic to exploit. To produce pure compounds from natural materials, the extraction of terpenes and terpenoids is of the most importance, being an area regarding eagerly for new technological developments (Martins et al., 2016).

The most used techniques to remove hydrocarbons from essential oils are vacuum and steam distillations, membrane processes, supercritical extraction, solvent (or liquid-liquid) extraction and chromatography. The solvent extraction used to remove terpenes and terpenoids is preferred, since this method requires less energy than processes such as distillation and supercritical fluid extraction, while retaining the most volatile aliphatic chemicals and preserving the organoleptic properties of the original oil (Oliveira et al., 2013).

In this work, 1-butyl-3-methylimidazolium acetate (BmimAc) was chosen to be tested as a separation agent. Previous studies have shown that the acetate anion showed a high selectivity according prediction by COSMO-RS (Conductor-like Screening Model for Real Solvents) and a nonpolar cation it is possible obtain high capacities values for separation between limonene/linalool. This IL showed a better result in the separation of linalool and limonene when compared to [C<sub>2</sub>mim][OAc] for instance (Lago et al., 2014; Martins et al., 2016).

To evaluate the behavior of solvent, a fast screening method is necessary to avoid the demanding experimental liquid-liquid equilibria assays. Solute-solvent interactions, selectivities and capacities can be derived from activity coefficients at infinite dilution. These can be determined from retention times using gas-liquid chromatography, and are related to the relative strength of intermolecular interaction of the solute with the ionic liquid (Martins et al., 2016).

Besides that, it is necessary to find a way to recycle the ionic liquids to minimize their cost in the process. Among all existing methodologies, the crystallization of water from aqueous solutions of ionic liquids proved to be a good option, being necessary to know the freezing point of the mixture (Noshadi and Sadeghi, 2018).

## 2.2. Activity coefficients measurements by gas chromatography

The chromatographic separation is achieved by the reversible formation of transient complexes between solutes and adsorption sites of a stationary phase. If one of two solutes forms a more stable complex, it will be retained in a chromatographic column longer than the second component that forms a less stable complex (Grushka and Grinberg, 2017). Through this technique, activity coefficients in binary liquid mixtures can be determined.

Activity coefficients are often estimated from a few experimental vapor-liquid equilibrium data for the mixtures by using some empirical (or semiempirical) excess Gibbs energy function. The excess functions provide a thermodynamically consistent method for interpolating and extrapolating limited binary experimental mixture data and for extending binary data to multicomponent mixtures (Poling et al., 2001).

The measurements of activity coefficients at infinite dilution are fundamental to provide information about the intermolecular energy between solvent and solute and through this, to assist the selection of solvents for liquid-liquid extraction or separation agents in distillation, allowing also to determine thermodynamic functions at infinite dilution such as gas-liquid partition coefficients, partial molar excess Gibbs free energy, enthalpy and entropy (Królikowska and Orawiec, 2016).

The activity coefficients at infinite dilution can be determined using gas-liquid chromatography (GLC) by measuring the retention times of the solutes, being the lowest values obtained by solutes with smaller interaction with the stationary phase. In this technique, the chromatography column is coated with the ionic liquid and the solutes introduced with a carrier gas. The GLC method works for solutes that are retained by the IL more strongly than by the carrier gas (usually helium). The solutes retention times are a measure of the strength of interaction between the solute and the ionic liquid, resulting from complex interactions such as hydrogen bonding,  $\pi - \pi$ , and  $\sigma - \pi$  interactions (Martins et al., 2015, 2016).

Solute-solvent interactions, selectivities and capacities can be derived from activity coefficients at infinite dilution relating the relative strength of intermolecular interaction of the solute with the ionic liquid. The use of gas-liquid chromatography avoids performing a large number of experimental liquid-liquid extractions; so, to fully exploit the ILs potential in extraction and separation processes of terpenes, screening methods to evaluate the best solvents are necessary (Martins et al., 2016).

### 2.2.1. Methodology

The methodology selected in this work was followed by Martins et al, (2015) that was already used to analyze organic family solutes such as alkenes, alkynes, ketones, ethers, esters, alcohols, aromatic hydrocarbons, and water in several ionic liquids (Martins et al., 2015). The organic solutes that were selected had boiling points between 304.12 and 428.76 K, avoiding decomposition of the IL. Values were determined temperature intervals, ranging between 398.15 and 428.15 K and from 358.15 to 388.15 K for alcohols and water (Martins et al., 2015).

For the preparation of ILs, they were dried under vacuum, and after their purity was checked by NMR. The Karl Fischer titration method was used to determine the water content of the dried ILs. For the preparation of the samples, they were dissolved in dry methanol and titrated. The organic solutes were not purified once GLC technique separates impurities in the column, and the water used was filtered and distilled, presenting a final mass fraction purity higher than 0.999 (Martins et al., 2015).

The activity coefficients at infinite dilution were determined using a gas chromatograph equipped with a heated on-column injector and a thermal conductivity detector (TCD). The inlet pressure  $P_i$ , was measured using a pressure gauge installed on the GC and the outlet pressure  $P_0$  was measured by one Gas Flow Meter placed outside, after the detector. Helium was used as the carrier gas and the exit gas flow rates were measured using the same Gas Flow Meter. The inlet pressure varied according to the type of solute injected. Data were collected and processed using the TotalChrom Workstation software. More details about the GLC method were previously presented in detail by Domanska et al. (2011).

The column packing containing between 45 and 55% of the IL stationary phase, each IL was dissolved in methanol and dispersed in Chromosorb, and then the mixture was shaken (Martins et al., 2015).

A series of ionic liquids were already tested for the separation of compounds in a simplified, modelled citrus essential oil consisting of a mixture of limonene (a representative terpene used in biodegradable solvents) and linalool (a representative oxyterpene used in perfumery industries) (Lago et al., 2011). Table 1 compiles a list of research works using IL as a separating agent for terpenes fractionation as well as those already studied for the infinite dilution activity coefficients.

**Table 1:** Results found in literature about the behavior of ILs for extraction and separation of terpenes.

| Ionic liquid   | Reference                                 | Reasons   |
|--|---|---|
| 1-Butyl-3-methylimidazolium acetate                                  | Lago et al. (2014); Martins et al. (2016) | A good separation agent for the mixture linalool + limonene. This IL was also studied by Martins et al. [27], where selectivities and capacities were simulated by COSMO-RS for several binary mixtures of terpenes. The results are among the best pointed by COSMO-RS.  |
| 1-Butyl-3-methylimidazolium chloride                                 | Martins et al. (2015), (2016)             | The $\gamma$ at infinite dilution were measured for several terpenes. The selectivities found were interesting for some mixtures, but among the poorest for the pair $\alpha$ -pinene/ $\beta$ -pinene. This IL was also studied as separation agent for organic solvents, showing very promising results for important purification steps in the fuel industry |
| 1-Butyl-3-methylimidazolium bis(trifluoromethyl-sulfonyl)imide       | Martins et al.(2016)                      | The selectivities and capacities were simulated by COSMO-RS for several binary mixtures of terpenes. The results are the third poorest among the four ILs studied.  |
| 1-Butyl-3-methyl-imidazolium methanesulfonate                        | Martins et al. (2016)                     | The $\gamma$ at infinite dilution were experimentally measured for several terpenes. The selectivities found were among the poorest reported by the authors.  |
| 1-Butyl-3-methylimidazolium trifluoromethanesulfonate                | Martins et al. (2016)                     | The $\gamma$ at infinite dilution were experimentally measured for several terpenes. The selectivities found here were the best, in general, including for the $\alpha$ -pinene/ $\beta$ -pinene pair.  |
| 1-Ethyl-3-methylimidazolium 2-(2-methoxyethoxy) ethylsulfate         | Francisco et al. (2010)                   | It does not have high selectivity and high solute distribution ratio for the mixture linalool + limonene.   |
| 1-Ethyl-3-methyl-imidazolium acetate                                 | Lago et al. (2014)                        | A good separation agent for the mixture linalool + limonene.  |
| 1-Ethyl-3-methylimidazolium ethyl sulfate                            | Arce et al. (2007)                        | It does not have high selectivity and high solute distribution ratio for the mixture linalool + limonene.   |
| 1-Ethyl-3-methylimidazolium bis(trifluoromethyl-sulfonyl)imide       | Lago et al. (2011)                        | It does not have high selectivity and high solute distribution ratio for the mixture linalool + limonene.   |
| 1-Ethyl-3-methylimidazolium methanesulfonate                         | Arce et al. (2006)                        | It does not have high selectivity. The solute distribution ratios are good in the linalool rich phase.  |
| 1-Hexyl-3-methylimidazolium bis(trifluoromethyl sulfonyl)imide       | Lago et al. (2011)                        | It does not have high selectivity and high solute distribution ratio for the mixture linalool + limonene.   |
| Trihexyltetradecylphosphonium acetate                                | Martins et al. (2016)                     | The selectivities and capacities were simulated by COSMO-RS for several binary mixtures of terpenes. The results are among the best pointed by COSMO-RS.  |
| Trihexyltetradecylphosphonium bis 2,4,4-(trimethylpentyl)phosphinate | Martins et al. (2016)                     | The selectivities and capacities were simulated by COSMO-RS for several binary mixtures of terpenes. The selectivities found here were the best, in general, but were lower for the $\alpha$ -pinene/ $\beta$ -pinene fractionation.  |

### 2.2.2. Theoretical principles

The following equation will be used in this work to calculate the activity coefficient at infinite dilution ( $\gamma_{13}^{\infty}$ ) (Martins et al., 2015):

$$\ln \gamma_{13}^{\infty} = \ln \left( \frac{n_3 RT}{V_N P_1^*} \right) - \frac{P_1^* (B_{11} - V_1^*)}{RT} + \frac{P_0 J_2^3 (2B_{12} - V_1^{\infty})}{RT} \quad (1)$$

Being  $n_3$  the number of moles of solvent on the column packing,  $T$  the column temperature,  $V_N$  the net retention volume of the solute,  $P_1^*$  the saturated vapor pressure of the solute at temperature  $T$ ,  $B_{11}$  the second virial coefficient of the pure solute,  $V_1^*$  the molar volume of the solute,  $P_0$  the outlet pressure,  $J_2^3$  a pressure correction term,  $B_{12}$  the mixed second virial coefficient of the solute and the carrier gas (where 2 refers to the carrier gas, helium) and  $V_1^{\infty}$  the partial molar volume of the solute at infinite dilution in the solvent. The values of  $B_{12}$  were calculated using the Tsonopolous equation (Domanska et al., 2016). The pressure correction term  $J_2^3$  is given by:

$$J_2^3 = \frac{2 \left( \frac{P_i}{P_0} \right)^3 - 1}{3 \left( \frac{P_i}{P_0} \right)^2 - 1} \quad (2)$$

and the net retention volume of the solute,  $V_N$  can be calculated by the following equation:

$$V_N = (J_2^3)^{-1} U_0 (t_R - t_G) \quad (3)$$

where  $t_R$  and  $t_G$  are the retention times, for the solute and an unreturned gas (air), respectively, and  $U_0$  is the column outlet volumetric flow rate (Wlazło et al., 2016).

It is also possible to calculate some important partial molar excess thermodynamic functions, such as the excess Gibbs free energy  $\bar{G}_m^{E,\infty}$ , excess enthalpy  $\bar{H}_m^{E,\infty}$  and excess entropy  $\bar{S}_m^{E,\infty}$ , because the activity coefficients at infinite dilution were determined as a function of temperature. The following equations allow the partial molar excess properties to be estimated due to the fact the experimental activity coefficients were measured at infinite dilution (Martins et al., 2015).

$$\bar{G}_m^{E,\infty} = RT \ln(\gamma_{13}^{\infty}) \quad (4)$$



$$\bar{H}_m^{E,\infty} = R \left( \frac{\partial \ln(\gamma_{13}^\infty)}{\partial \left(\frac{1}{T}\right)} \right)_{p,\underline{x}} \quad (5)$$

$$\bar{S}_m^{E,\infty} = \frac{\bar{H}_m^{E,\infty} - \bar{G}_m^{E,\infty}}{T} \quad (6)$$

Subscripts  $p, \underline{x}$  indicate isobaric and constant composition conditions, respectively.

The gas-liquid partition coefficient  $K_L = (c_1^L/c_1^G)$  for a solute, partitioning between a carrier gas and an ionic liquid, was calculated from the solute retention and is given by:

$$\ln(K_L) = \ln \left( \frac{V_n \rho_3}{m_3} \right) - \frac{P_0 J_2^3 (2B_{12} - V_1^\infty)}{RT} \quad (7)$$

where  $\rho_3$  is the density of the IL,  $m_3$  is the mass of the IL, and  $V_1^\infty$  is the partial molar volume of the solute at infinite dilution (Wlazło et al., 2016).

The way to identify the best separating agents for a certain separation problem is to use parameters such as selectivity  $S_{ij}^\infty$  between the solutes  $i$  and  $j$ , and the capacity  $k_j^\infty$  of the separation process defined as:

$$S_{ij}^\infty = \frac{\gamma_i^\infty}{\gamma_j^\infty} \quad (8)$$

$$k_j^\infty = \frac{1}{\gamma_j^\infty} \quad (9)$$

being  $j$  the solute that presents the smallest infinite dilution activity coefficient in the solvent (Martins et al., 2015).

The theoretical principles described above were developed by Everett, (1965) and Cruickshank et al. (1967), being valid when an infinitesimal amount of solute sample is introduced into a GLC column with a non-volatile stationary phase (Domanska et al., 2011; Martins et al., 2015).

### 2.3. Freezing point measurements

Considering that a small amount of solute is diluted in a liquid solvent and that the temperature of the mixture is decreased, a temperature  $T_f$  is reached when the pure solvent begins to separate out as a solid. This temperature is lower than the melting point of the pure solvent,  $T_m$ . Due to the

addition of a solute, it is important to estimate the freezing point depression ( $\Delta T = T_m - T_f$ ) (Sandler, 1999).

Here the interest is, from a thermodynamic point of view, the equilibrium between a solid and a liquid mixture that is concentrated in that component (Sandler, 1999). To understand the freezing point depression phenomenon, it is necessary to observe the formation of a pure solid from a liquid mixture. The equilibrium condition when the first pure crystal forms from the liquid mixture is given by (Sandler, 1999):

$$f_1^S(T_f, P) = f_1^L(T_f, P, \underline{x}) = x_1 \gamma_1(T_f, P, \underline{x}) f_1^L(T_f, P) \quad (10)$$

where  $f_1^S$  is the fugacity in a solid phase that varies with temperature and pressure ( $P$ ),  $f_1^L$  is the fugacity of the pure compound 1 in the liquid state at the temperature and pressure of the system. Additionally,  $x_1$  refers to the mole fraction of component 1, that precipitates as a solid from the liquid solution, being  $\gamma_1$  its activity coefficient, that depends on the temperature, pressure and composition. Equation 1 assumes that the solid phase is pure solid and uses the fact that the composition of the liquid phase is not significantly changed by the appearance of a very small amount of solid phase (Sandler, 1999).

To obtain the freezing point depression, the extent to which a solid is soluble in a solvent must be considered. Equation 2 is a combination between Equation 1 and expression for the solubility of a solid in a liquid, resulting in:

$$\begin{aligned} \ln \gamma_1 x_1 &= \ln \frac{f_1^S(T_f, P)}{f_1^L(T_f, P)} = -\frac{\Delta H^{\text{fus}}(T_m)}{R} \left[ \frac{T_m - T_f}{T_m T_f} \right] - \frac{1}{RT_f} \int_{T_m}^{T_f} \Delta C_p dT + \frac{1}{R} \int_{T_m}^{T_f} \frac{\Delta C_p}{T} dT \\ &= \frac{-\Delta H^{\text{fus}}(T_m)}{R} \left[ \frac{T_m - T_f}{T_m T_f} \right] - \frac{\Delta C_p}{R} \left[ 1 - \frac{T_m}{T_f} + \ln \left( \frac{T_m}{T_f} \right) \right] \end{aligned} \quad (11)$$

Equation 2 is the general equation that describes the freezing-point depression of a solvent, being  $-\Delta H^{\text{fus}}(T_m)$  the heat of fusion at the normal melting point temperature,  $R$  is the universal gas constant and  $\Delta C_p$  is the heat capacity change upon melting (Sandler, 1999).

If  $T_m$  and  $T_f$  are very close, then Equation 2 can be simplified:

$$\ln \gamma_1 x_1 \cong \frac{-\Delta H^{\text{fus}}(T_m)}{R} \left( \frac{T_m - T_f}{T_m T_f} \right) \cong \frac{-\Delta H^{\text{fus}}(T_m)}{RT_m^2} (T_m - T_f) \quad (12)$$

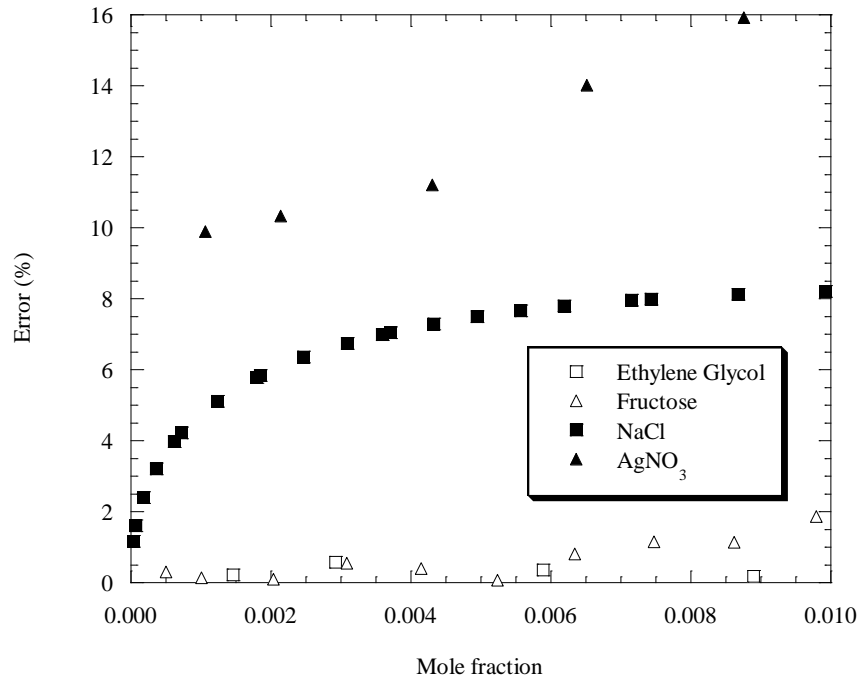
Rearranging:

$$-\frac{RT_m^2}{\Delta H^{\text{fus}}(T_m)} \ln \gamma_1 x_1 = (T_m - T_f) = \Delta T \quad (13)$$

If we consider a case of very diluted solutes, then  $\gamma_1 \sim 1$ , and  $\ln x_1 = \ln(1 - x_2) \sim -x_2$ , so the freezing point depression equation may be simplified to:

$$\Delta T = (T_m - T_f) \cong \frac{RT_m^2}{\Delta H_{fus}(T_m)} x_2 \quad (14)$$

So, Equation 5 can be called the simplified equation for a freezing point depression of a solvent (Sandler, 1999). However, using this equation different performances are obtained for non-electrolyte and electrolyte solutions. Figure 1 shows the relative percent deviation obtained for the representation of freezing point depression for diluted aqueous solutions of D-fructose, ethylene glycol, NaCl or AgNO<sub>3</sub> (Pinho and Macedo, 2004).



**Figure 1.** Relative percent deviations obtained for the representation of freezing point depression for non-electrolyte and electrolyte solutions (Pinho and Macedo, 2004).

Note that for the NaCl and AgNO<sub>3</sub> aqueous solutions, the deviations are much more pronounced than for non-electrolyte systems. The results for the non-electrolytes can be attributed to the fact that they are very diluted, forming an ideal solution. However, when NaCl dissolves in water, it dissociates into chloride and sodium ions, and the interaction between ions in solution is effective over a much greater distance than the interaction between neutral solute particles such as non-

electrolyte systems. So, the previous equation cannot give a reliable result, even for very diluted electrolyte solutions (Pinho and Macedo, 2004).

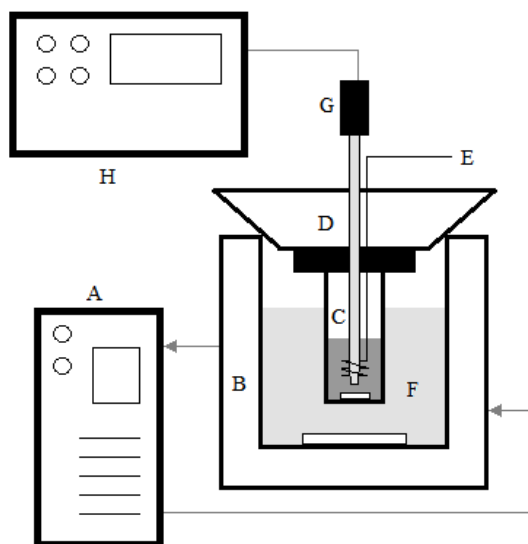
Thus, corrections to the ideal behavior consider the activity coefficient in order to obtain trustworthy values of  $\Delta T$ . From the thermodynamic condition for equilibrium it is possible to obtain (Pinho and Macedo, 2004):

$$\ln \gamma_1 x_1 = - \frac{\Delta H^{\text{fus}}(T_m)}{R} \left( \frac{1}{T_m} - \frac{1}{T_f} \right) \quad (15)$$

Now it is possible to calculate  $\Delta T$  solving Equation 6. However, the description of the physical chemistry of any mixture depends greatly on the available experimental data. In this way, the experimental measurement of the freezing point depression is of great help for technical applications as well as for validating theoretical methodologies. The next three sections explore techniques available to perform such measurements. The methodology used in this work was DSC.

### 2.3.1. Methodology I - Beckmann apparatus

The Beckmann apparatus can be used for the accurate measurement of water activity or freezing point depression, having a good repeatability. Liu et al. (2017) used it to measure the water activity in aqueous solutions of the ionic liquid 1-ethyl-3-methylimidazolium acetate. A schematic illustration of the equipment can be seen in Figure 2.



**Figure 2.** Illustration of the Beckmann equipment used by Liu et al. (2017) and Arshad et al. (2013) to measure the freezing point depression (adapted from Liu et al. (2017)): A, thermostatic bath; B, cooling jacket; C, sample glass with magnetic stirrer; D, rubber stopper with sample glass

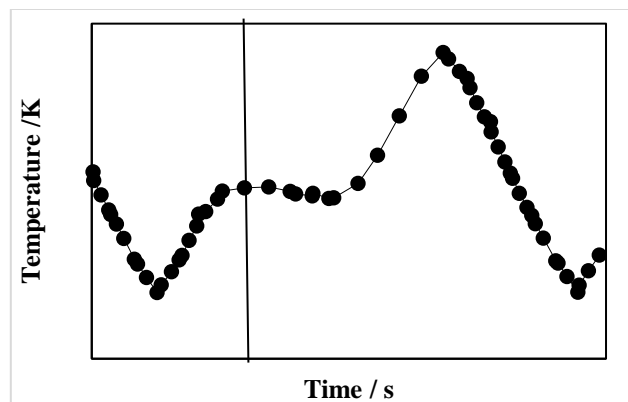
lid; E, device for manual stirring; F, ethanol bath for control temperature with magnetic stirrer; G, Pt100 thermometer; H, data acquisition unit.

In A, there is a thermostatic bath with ethanol as refrigerant and the lowest temperature obtainable is about 225 K. For samples with freezing points lower than this, liquid nitrogen was used as refrigerant. In C, the sample glass of the ionic liquid solution was placed with the magnetic stirrer. The temperature control was made using the ethanol bath (F) or liquid nitrogen maintained by a cooling jacket (B). A manual stirring device was used together with a continuous magnetic stirrer to ensure a homogeneous sample temperature during the measurement (E). The sample temperature was recorded by a data acquisition unit (H) using a Pt100 thermometer (G). The data acquisition unit was calibrated with seven different sodium chloride solutions. Deionized water was used for the preparation of sample solutions and as blank control. All the samples were weighed by an analytical balance with an accuracy of  $\pm 0.1$  mg (Liu et al., 2017).

Every sample of calibration was repeated 10 times for freezing point measurements, and the standard deviation did not exceed 0.02 K. The samples of the IL solutions were measured 5 times each (Liu et al., 2017).

Following the methodology with the Beckmann apparatus, Arshad et al. (2013) studied aqueous solutions of two amines, 2-(diethylamino)ethanol (DEEA) and 3-(methylamino)propylamine (MAPA), varying the temperature in the thermostatic ethanol bath that was kept about 5 – 15 °C below the expected freezing point (A). The calibration of the data acquisition unit (H) was also made with aqueous NaCl, following the same steps of Liu et al. (2017).

Figure 3 provides an example of temperature curves using the Beckmann apparatus. The temperature of the controlled temperature bath was adjusted to approximately 5 K below the expected freezing point of the sample, next was placed in a sample glass which was closed with a lid attached to the rubber stopper. The sample glass was then lowered into the controlled temperature bath. Ice formation was registered at the rise of the sample temperature as the latent heat of fusion of liquid water was released. From the start of the experiment the sample is cooled. Hereafter the temperature rises abruptly to approximately due to ice formation. The freezing point is recorded as indicated by the vertical line in Figure 3.



**Figure 3.** Temperature profile in a freezing point measurement. Adapted from Fosbøl et al. (2011).

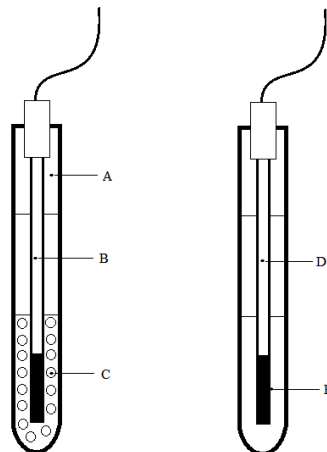
After, the temperature drops slightly due to a change of the water concentration in the liquid phase from freezing out of ice. The ice in the sample is melted by placing the glass in an ethanol bath at room temperature.

This was obtained by “heating” a few seconds and visually inspecting the sample. Close to the point where all ice was melted, the heating could be done by holding the sample glass in the air while stirring and carefully watching the small remaining crystals. This way microscopic ice crystals were kept in solution as seed crystals by not heating the solution too much. It limits the subcooling during ice formation in the next measurement. The freezing point depression of aqueous monoethanolamine (MEA), methyl diethanolamine (MDEA), and MEA-MDEA solutions, the aqueous MEA-MDEA system and MEA/MDEA were successfully determined using the Beckmann apparatus (Fosbøl et al., 2011).

### 2.3.2. Methodology II – Heriot-Watt University apparatus

Haghighi et al. (2008) measured the freezing point depression of six binary aqueous solutions containing NaCl, CaCl<sub>2</sub>, MgCl<sub>2</sub>, KOH, ZnCl<sub>2</sub> or ZnBr<sub>2</sub>, and four aqueous ternary solutions (NaCl–KCl, NaCl–CaCl<sub>2</sub>, KCl–CaCl<sub>2</sub> and NaCl–MgCl<sub>2</sub>) using a differential temperature technique.

The samples were prepared gravimetrically, and deionized water was used. The equipment is comprised of two cells, each containing a platinum resistance temperature - PRT (B, D, E), surrounded by an aluminum sheath, placed in a controlled temperature bath. One cell contains the bath fluid (as a reference fluid) and the second cell contains the aqueous electrolyte solution. A scheme is shown in Figure 4 (Haghighi et al., 2008).



**Figure 4.** Schematic illustration of a freezing point apparatus (Haghighi et al., 2008): A, PTFE - poly(tetrafluoroethylene) sealing sleeve; B, Sample PRT; C, Packed, saturated sample; E, Reference PRT and D, PRT sensitive region.

Initially, the temperature of the test sample is reduced sufficiently to promote ice formation, being determined by a rise in the sample temperature as the latent heat of formation is released. The bath temperature is increased at a constant rate and the temperatures of the bath, reference cell and sample cell are recorded. The temperature of the sample will continue lower than the bath temperature as thermal energy is required to melt the ice. When the last crystal of ice has melted, the sample temperature will converge to the bath temperature. The point at which the bath and sample temperatures begin to converge can be easily identified as the freezing point of the sample or ice melting point (Haghighi et al., 2008).

The temperature of each probe is measured during the ramp (either heating or cooling) by recording the voltage generated across each PRT by a constant current generator (Haghighi et al., 2008).

### 2.3.3. Methodology III - Differential scanning calorimetry

Differential Scanning Calorimetry (DSC) measures the change of the difference in the heat flow rate between the reference sample, and the sample, while they are subjected to a controlled temperature program. This method is used because the DSC is a dynamic procedure, while a phase diagram indicates an equilibrium state, and because of ability to provide detailed information about both the physical and energetic properties of a substance (Clas et al., 1999).

Noshadi and Sadeghi (2018) measured the solid-liquid equilibrium data of binary mixtures of a carboxylic acid and water. Samples of formic acid, acetic acid, propionic acid or butyric acid were also characterized by DSC. Nitrogen gas was used as a purge gas and as a protective gas with.

Samples were weighted and sealed in an aluminum pan. An empty aluminum pan was used as reference during the measurements. Before the analysis, the heat flow was calibrated using the standards indium and bismuth and by the onset temperatures measured at three different heating rates, 1, 5, and 10 K min<sup>-1</sup>.

Thermal transition was determined using the following sequence, with heating/cooling rate of 5 K·min<sup>-1</sup>. The sample was: i) cooled to a temperature at least 50 K below the melting point of the component with the smallest melting temperature; ii) held at that temperature for 5 min; iii) warmed until 25 K above the melting point of the component with the highest melting temperature; iv) again cooled up to the desired temperature; v) held at that temperature for 5 min; vi) warmed until 298 K. The measurements were carried out for each concentration (Noshadi and Sadeghi, 2018).

Noshadi and Sadeghi (2018) compared the DSC methodology with other techniques reported in the literature, including the Beckmann apparatus and concluded that the results are consistent with literature data, being possible to apply this method to measure the freezing point. This methodology was selected to use in this work due to advantages and availability of equipment.

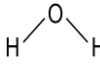





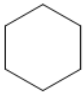
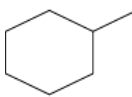
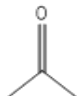
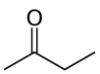

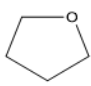
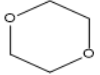
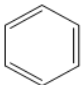
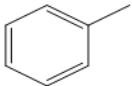
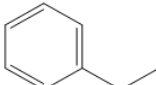
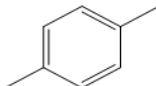
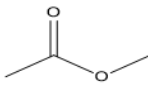
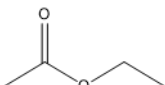
## Chapter 3. Experimental infinite dilution activity coefficients

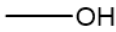
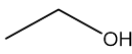
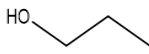
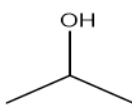
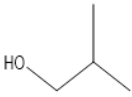

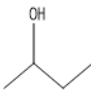

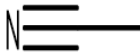
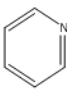
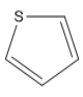
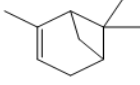
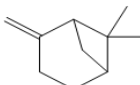
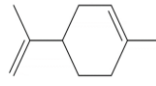
### 3.1. Chemicals

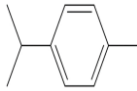
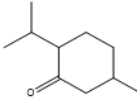
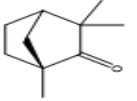
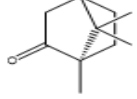
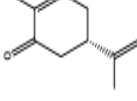
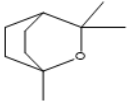
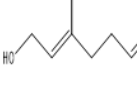
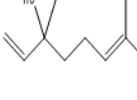
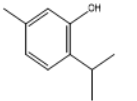

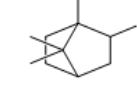
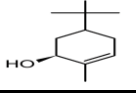
The chemical structure, source, boiling point temperature (TBP) and mass fraction purity indicated by the supplier are presented in Table 2. The solutes tested were organized by chemical family.

**Table 2.** Name, structure, supplier, boiling point (TBP) and purity of the investigated solutes.

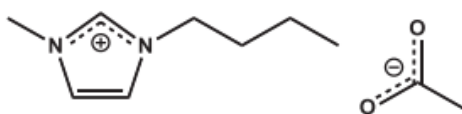
|         | Chemicals | Structure  | Source  | TBP (K) | Mass fraction purity |
|---------|-----------|--|---------|---------|----------------------|
|         | Water     |   |         | 373.15  |                      |
| Alkanes | Octane    |  | Aldrich | 398.75  | ≥ 0.990              |
|         | Nonane    |  | Aldrich | 424.15  | ≥ 0.990              |
|         | Decane    |  | Aldrich | 447.25  | ≥ 0.990              |

|                       |                              |  |         |        |              |
|-----------------------|------------------------------|--|---------|--------|--------------|
| Cycloalkanes          | Cyclohexane                  |     | Aldrich | 354.15 | $\geq 0.990$ |
|                       | Methylcyclohexane            |     | Aldrich | 374.15 | $\geq 0.990$ |
| Ketones               | Propan-2-one (Acetone)       |     | Aldrich | 329.15 | $\geq 0.999$ |
|                       | 2- Butanone                  |     | Aldrich | 352.79 | $\geq 0.990$ |
| Ethers                | Ethoxyethane (Diethyl ether) |     | Aldrich | 307.75 | $\geq 0.999$ |
| Cyclic Ethers         | Oxolane (THF)                |     | Aldrich | 339.15 | $\geq 0.999$ |
|                       | 1,4-Dioxane                  |    | Aldrich | 374.15 | $\geq 0.998$ |
| Aromatic Hydrocarbons | Benzene                      |   | Aldrich | 353.25 | $\geq 0.998$ |
|                       | Toluene                      |   | Aldrich | 383.75 | $\geq 0.998$ |
|                       | Ethylbenzene                 |  | Aldrich | 409.15 | $\geq 0.998$ |
|                       | <i>p</i> -Xylene             |  | Aldrich | 411.55 | $\geq 0.990$ |
| Esters                | Methyl acetate               |   | Aldrich | 330.25 | $\geq 0.998$ |
|                       | Ethyl acetate                |  | Aldrich | 350.25 | $\geq 0.998$ |

|              |   |  |               |              |              |
|--------------|---|--|---------------|--------------|--------------|
| Alcohols     | Methanol  |     | Aldrich       | 337.85       | $\geq 0.999$ |
|              | Ethanol   |     | Aldrich       | 351.52       | $\geq 0.998$ |
|              | Propan-1-ol   |    | Aldrich       | 370.15       | $\geq 0.999$ |
|              | Propan-2-ol   |     | Fluka         | 355.65       | $\geq 0.999$ |
|              | 2-Methyl-propan-1-ol  |     | Aldrich       | 381.15       | $\geq 0.995$ |
|              | Butan-1-ol  |    | Aldrich       | 390.85       | $\geq 0.998$ |
|              | Butan-2-ol  |     | Aldrich       | 373.15       | $\geq 0.995$ |
|              | 2-Methyl-propan-2-ol ( <i>tert</i> -Butanol)  |   | Aldrich       | 355.15       | $\geq 0.997$ |
| Acetonitrile |  | Fluka  | 355.15        | $\geq 0.999$ |              |
| Pyridine     |  | Aldrich  | 388.15        | $\geq 0.998$ |              |
| Thiophene    |  | Aldrich  | 357.15        | $\geq 0.990$ |              |
| Terpenes     | $\alpha$ -pinene  |   | Sigma-Aldrich | 429.29       | 98%          |
|              | $\beta$ -pinene   |   | Sigma-Aldrich | 439.19       | 99%          |
|              | R(+)-Limonene   |  | Aldrich       | 449.15       | 97%          |

|            |   |   |               |        |        |
|------------|---|---|---------------|--------|--------|
|            | p-Cymene  |    | Aldrich       | 450.15 | 99%    |
| Terpenoids | (-)-menthone  |    | Fluka         | 483.15 | ≥99%   |
|            | (1R)-(-)-fenchone   |    | Aldrich       | 466.15 | ≥98%   |
|            | (1R)-(+)-camphor  |    | Aldrich       | 480.55 | 98%    |
|            | (S)-(+)-carvone   |    | Merck         | 504.15 | 96%    |
|            | Eucalyptol  |    | Aldrich       | 449.55 | 99%    |
|            | Geraniol  |   | Sigma-Aldrich | 503.15 | 98%    |
|            | Linalool  |  | Aldrich       | 470.15 | 97%    |
|            | Thymol  |  | Sigma         | 505.65 | ≥99.5% |
|            | α-pinene oxide  |  | Aldrich       | 489.51 | 97%    |
|            | (-)-borneol   |  | Fluka         | 485.80 | ≥99%   |
| Sobrerol   |  | Sigma-Aldrich   | 544.15        | ≥99%   |        |

The structure of the ionic liquid used in this work is presented below:



**Figure 5.** Chemical structure of 1-butyl-3methylimidazolium acetate BmimAc.

### 3.2 Experimental methodology selected in this work

The activity coefficients at infinite dilution were obtained using a CP-3380 Varian Gas Chromatograph (Figure 6), equipped with a heated on-column injector with temperature kept at 473.15 K for alkanes, cycloalkanes, ketones, ethers, cyclic ethers, esters, aromatic hydrocarbon, acetonitrile, pyridine and thiophene, and at 523.15 K for alcohols, terpenes and terpenoids. The temperature of the thermal conductivity detector (TCD) was set at 573.15 K for alcohols, terpenes and terpenoids, and at 523.15 K for the remaining solutes. The inlet pressure  $P_i$ , was measured using a pressure gauge installed on the GC and the outlet pressure  $P_o$ , was measured by an Agilent Precision Gas Flow Meter placed outside the GC, after the detector. Helium was used as the carrier gas.



**Figure 6.** GC used in this work.

Two columns were used to compare the values of the activity coefficients obtained in independent columns. The first column was tested with one solute from each family, and the second column was tested with all the solutes listed in Table 2. The column preparation was carried out at CICECO, Chemistry Laboratory of University of Aveiro, Portugal, according to the procedure described by Martins et al. (2015).

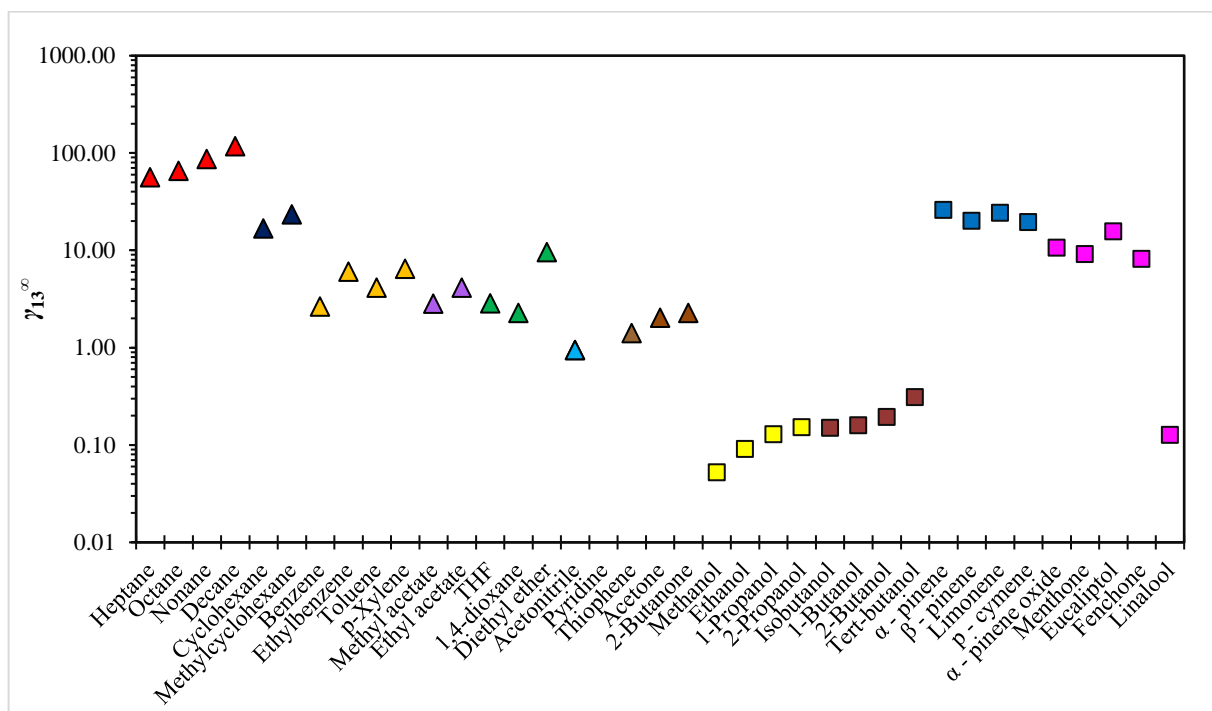
To measure the retention times, solutes were injected in the column in volumes of 0.2  $\mu\text{L}$ , to be at infinite dilution conditions. Each time, air was also injected, representing a non-retained

component. Absolute values of retention times varied between 0.363 to 155.7 min corresponding to heptane and linalool, respectively.

### 3.3 Experimental activity coefficient at infinite dilution

The average values of infinite dilution activity coefficients for several organic solutes are presented in Appendix Table A1. Each measurement was repeated twice in each column to guarantee the repeatability.

The measurements were carried out in the temperature range between 333.15 K and 393.15 K with intervals of  $T=10$  K for alkanes, cycloalkanes, ketones, ethers, cyclic ethers, esters, aromatic hydrocarbon, acetonitrile, pyridine and thiophene, with the exception of ethyl acetate that was not tested at 383.15 K. For terpenes and terpenoids, the temperature range was between 353.15 K to 403.15 K with intervals of  $T=10$  K due to their expected longer retention times, excepting *p*-cymene that was not measured at 393.15 K. For alcohols, the temperature range varied between 383.15 K and 403.15 K. To analyze the data, a comparison at fixed temperatures, 373.15 K and 403.15 K, is presented in Figure 7. Results for water, thymol, sobrerol, (-)-borneol, (S)-(+)-carvone, and camphor were not obtained in a reasonable amount of time, probably because of the high interaction between these solutes and the IL.

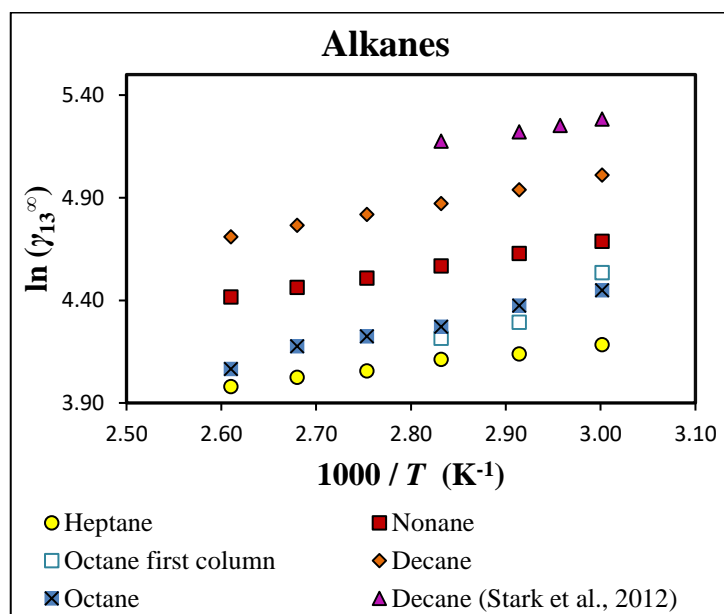


**Figure 7.** Activity coefficients at infinite dilution of several solutes in 1-butyl-3-methylimidazolium acetate, at T= 403.15 K represented by  $\square$  for alcohols, terpenes and terpenoids, and T= 373.15 K for the other organic compounds represented by  $\triangle$ .

A global analysis of Figure 7 shows that the alkanols, and linalool present the lowest  $\gamma_{13}^{\infty}$  values, indicating the highest interaction with the ionic liquid, what is expected since the ionic liquid has a highly polar anion which interacts better with polar solutes, as expected. The  $\gamma_{13}^{\infty}$  value of linalool was extrapolated to 403.15 K because at the measurements were carried out between 413.15 and 438.15 K with interval of 5 K. Other polar solutes such as thiophene, pyridine and acetonitrile present also low  $\gamma_{13}^{\infty}$  values.

The same occurred with water and the organic solutes that probably presented very high retention times, as mentioned previously. because their structure is more polar than those who presented lower retention times. The ability to accept hydrogen bonding in an ionic liquid is often connected with the basic character of its anion.

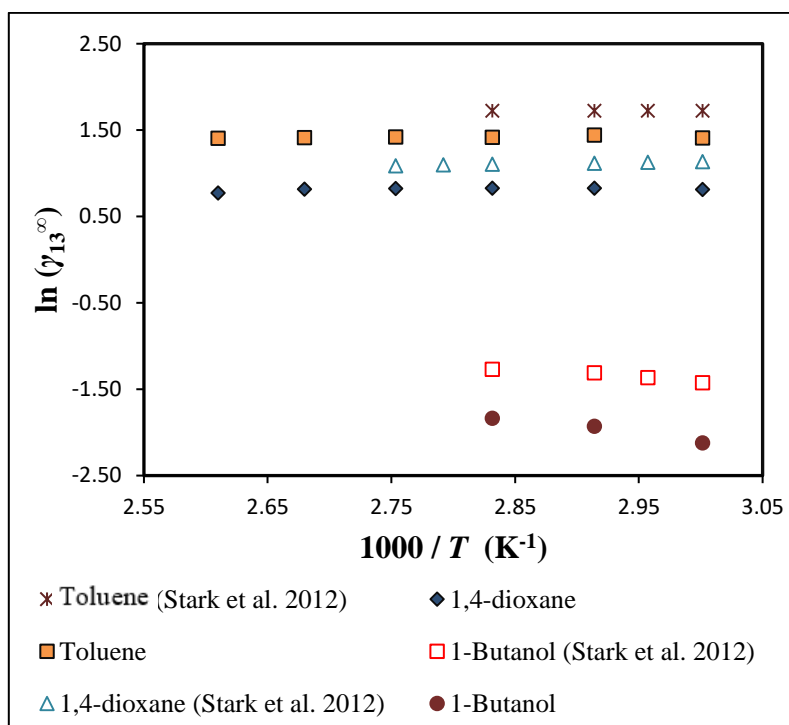
The opposite occurs with alkanes, cycloalkanes, hydrocarbons (terpenes), because they present the weakest interaction with the studied IL, being the less polar solvents. One factor that influences the values of  $\gamma_{13}^{\infty}$  is the chain length of solutes. Figure 8 presents one example of the temperature dependence of  $\gamma_{13}^{\infty}$  values of alkanes.



**Figure 8.** Activity coefficients at infinite dilution of alkanes.

The same behavior occurs with cycloalkanes, ketones, ethers, aromatic hydrocarbons, ethers and alcohols, in which the  $\gamma_{13}^{\infty}$  values increase with the increasing chain length. The results for the other families of compounds are presented in Appendix A1 to A6. This behavior is because the IL is very polar and by increasing the chain length, the polarity of the solute decreases, decreasing also the interaction between solute and solvent.

A similar study has been published by Stark et al. (2012) using the same methodology of gas chromatography with IL as stationary phase, for some solutes. The values compared with this work are presented in Figure 9.

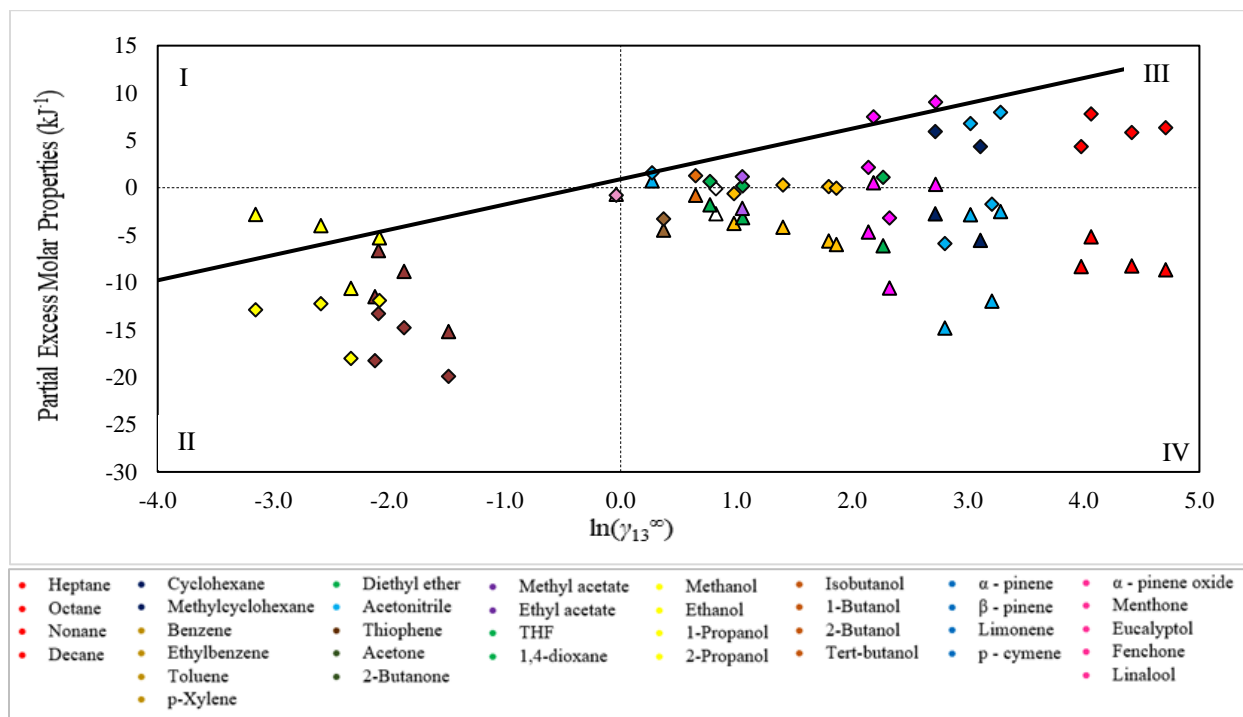


**Figure 9.** Comparison between results obtained in this work with values measured by Stark et al. (2012).

This comparison shows the same behavior. The values are not the same, but vary in the same order, presenting the same order of magnitude. This difference can be because of column packing; if it is more compact, the retention times tend to be higher. Still, there is a comparison between the data of decane obtained in this work and that by Stark et al. (2012), but because of the weak interaction with the IL, high values of  $\gamma_{13}^{\infty}$  were attained, not easily viewed in Figure 9. The values are presented in Appendix A1 and Figure 8, and as can be seen they present the same behavior.



The thermodynamic functions at infinite dilution (partial excess molar properties such as Gibbs energy, enthalpy, and entropy), were also calculated in order to provide more information about the interactions between the solutes and the IL, calculated through the  $\ln\gamma_{13}^{\infty}$  values (Figures 10 and 11). The  $\bar{G}_m^{E,\infty}$  is positive for alkanes, cycloalkanes, terpenes and terpenoids except for linalool, showing again the weak solutes-IL interaction. The  $\bar{G}_m^{E,\infty}$  is negative for alkanols and linalool, that are much lower for polar solvents due to the presence of delocalized electrons and the ability to form hydrogen bonds with the IL, indicating strong solute-IL interaction for these polar solutes. In Figures 10 and 11, the values of linalool were not plotted ( $\bar{G}_m^{E,\infty}$  was -6.57 kJ/mol but the value of  $\bar{H}_m^{E,\infty}$  is -306.77 kJ/mol and  $\bar{S}_m^{E,\infty}$  is -300.205 kJ/mol) to facilitate viewing the remaining results.

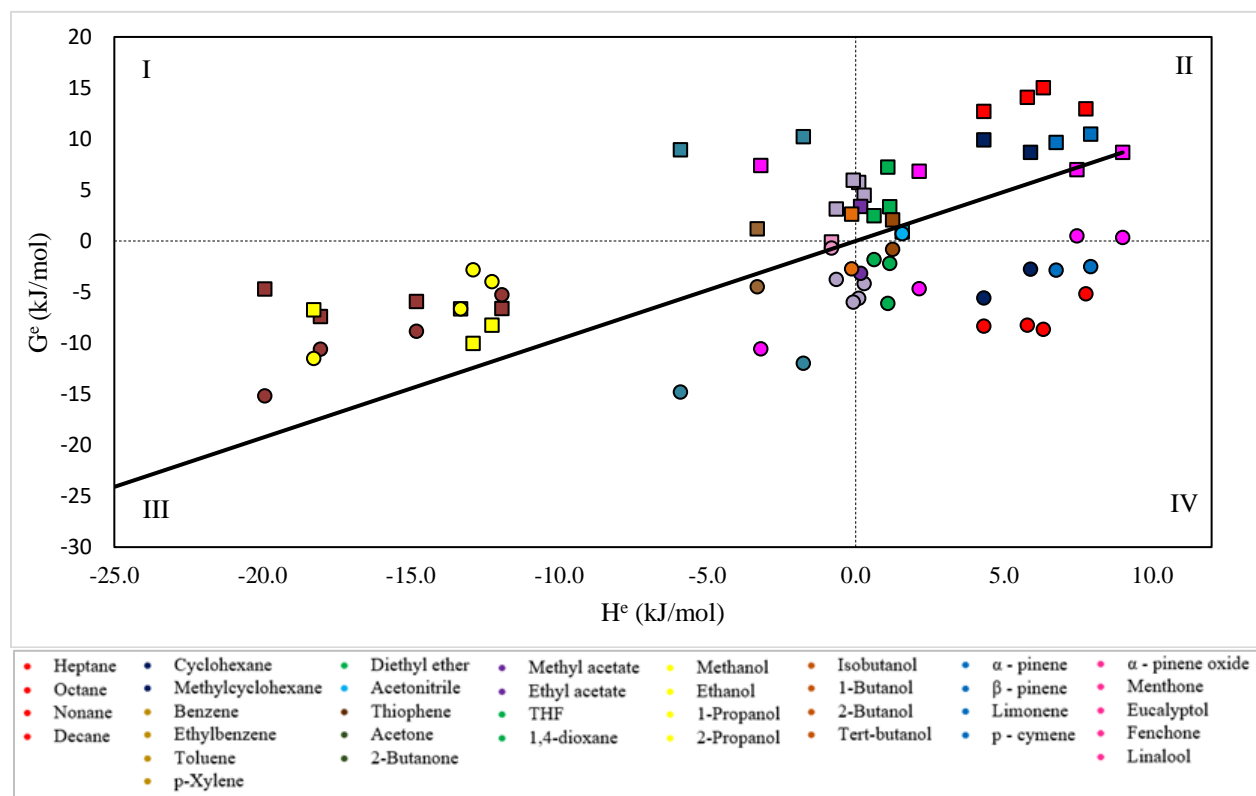


**Figure 10.** Partial molar excess properties as a function of the activity coefficients at infinite dilution of the organic solutes at 383.15 K. The line represents  $\bar{G}_m^{E,\infty}$  and the symbols correspond to:  $\diamond \bar{H}_m^{E,\infty}$  and  $\triangle T_{ref}\bar{S}_m^{E,\infty}$ .

The  $\bar{H}_m^{E,\infty}$ , calculated through the temperature dependence of  $\gamma_{13}^{\infty}$  exhibit negative values for alcohols, linalool,  $\alpha$ -pinene oxide, benzene, *p*-xylene, acetonitrile, thiophene and 2-butanone, indicating favorable interactions between the solute and the solvent, with the exception of alkanes, cycloalkanes,  $\alpha$ -pinene,  $\beta$ -pinene, eucalyptol, fenchone and menthone, all nonpolar compounds.

The  $\bar{S}_m^{E,\infty}$  presents negative values for almost solutes studied indicating their reorganization inside the ionic liquid phase, and often representing the dominance of entropic effect over the enthalpic one, but to menthone, pyridine and eucalyptol, the opposite behavior is observed.

In Figure 11, there are four different areas that can be distinguished to understand the molecular level interaction in this system.



**Figure 11.** Partial molar excess energies as a function of enthalpy of the organic solutes at 383.15 K and 353.15 K. The line represents linear ( $\bar{H}_m^{E,\infty}$  vs  $T_{ref}\bar{S}_m^{E,\infty}$ ). The  $\square$   $\bar{G}_m^{E,\infty}$  vs  $\bar{H}_m^{E,\infty}$  and the symbol  $\circ$  correspond  $\bar{H}_m^{E,\infty}$  vs  $T_{ref}\bar{S}_m^{E,\infty}$ .

Region (II) corresponds to the (IL + organic solutes) mixtures with positive deviation to Raoult's law,  $\gamma_{13}^\infty > 1$  and,  $\bar{G}_m^{E,\infty}$  and  $\bar{H}_m^{E,\infty}$  are positive. This region is mainly constituted by non-polar solutes such as alkanes, cycloalkanes, some terpenes ( $\alpha$ -pinene,  $\beta$ -pinene), an ether terpenoid (eucalyptol) and a ketone terpenoid (menthone), that presented no affinity with IL. This low interaction can lead to the formation of an immiscible mixture and, consequently, to phase separation.

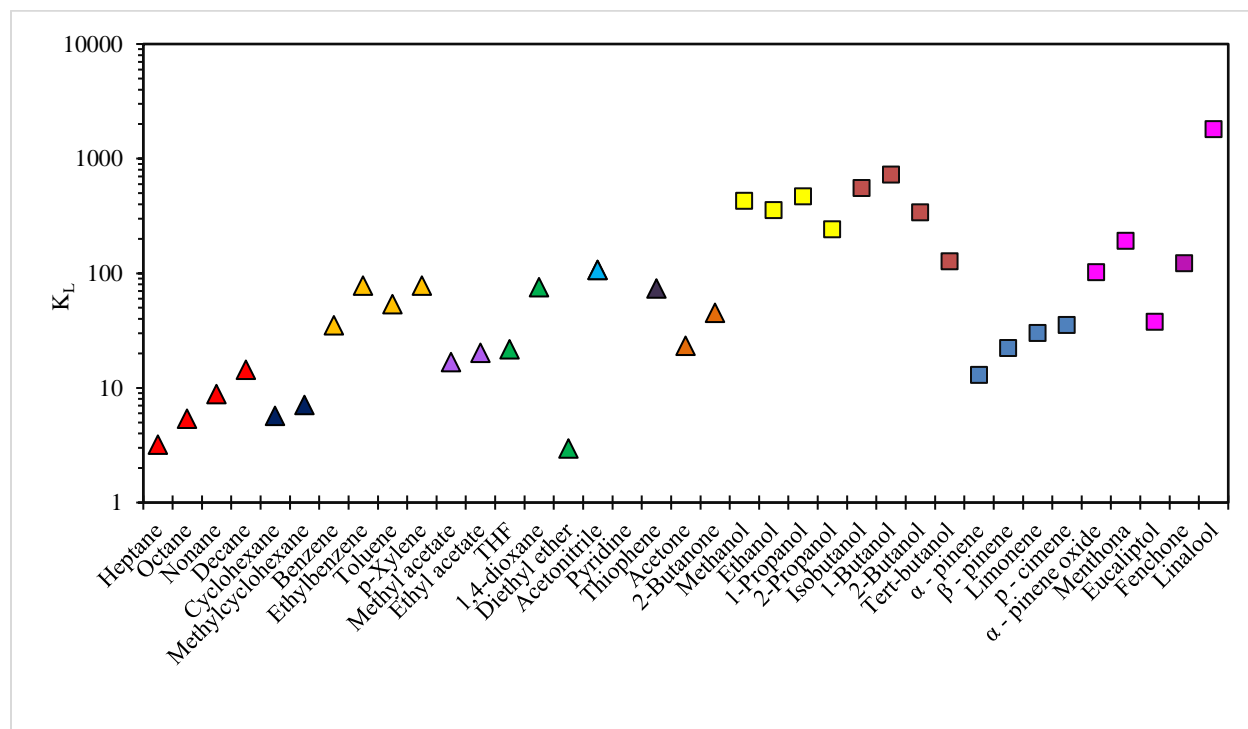
Region (III) corresponds to the system with negative deviation from Raoult's law,  $\gamma_{13}^\infty < 1$  that is related to a spontaneous dissolution of organic solutes in the IL. This region is constituted by polar

solutes such as alcohols, due to their strong polarity, highlighting the lower value of linalool that is not present in Figure 11, as explained before.

Region (IV) presents  $\gamma_{13}^{\infty} > 1$ ,  $\bar{S}_m^{E,\infty}$  and  $\bar{H}_m^{E,\infty} < 0$ . For some solutes  $\bar{G}_m^{E,\infty}$  is close to 0 such as acetonitrile, while the enthalpic and entropic cancel each other. We can compare region (IV) with region (II), in which the dominance of the entropic term over the enthalpic is evident; the opposite happens when the interaction between the solute and IL are strong (I and III), the enthalpic effect is always dominant.

When all the partial excess molar properties studied are negative, revealing that the hydrogen bonding between organic solutes and the IL anion is much stronger than hydrogen bonding between solute and solute or (IL + IL) molecules, showing an exothermic mixing behavior.

Now, to compare the affinity of the solute to both phases (gas + liquid), the  $K_L$  partition coefficients were calculated. The values of the IL density previously reported by Almeida et al. (2012), between 283.15 and 363.15 K, were used. The results of  $K_L$  are presented in Figure 12.



**Figure 12.** Experimental (gas + liquid) partition coefficients,  $K_L$ , for organic solutes in the ILs studied. The  $\triangle$  correspond the  $K_L$  values at 373.2 K and  $\square$  correspond at 403.5 K.

Assuming an ideal gas phase, the gas-liquid partition coefficients can be used to understand the terpenes and terpenoids extraction using IL for example, and their subsequent evaporation in order

to recover the IL, at low pressures (Martins et al., 2015). In Figure 12, the  $K_L$  increases with the alkyl chain in alkanes. The highest values are observed for alcohols and terpenoids such as geraniol and linalool, whereas the lowest values are observed for diethyl ether and heptane.

In Appendix A7, the variation of  $K_L$  with temperature is presented. As can be observed,  $K_L$  decreases with increasing temperature for all solutes, and increases with the alkyl chain for alkanes, cycloalkanes, aromatic hydrocarbons, ketones and esters. This result is consistent with previous analyses, since higher  $K_L$  value corresponds to larger affinities of the solute to the liquid phase.

Finally, we will discuss about selectivities and capacities that provide information about the performance of IL as solvent in several chemical engineering applications (Martins et al., 2015). A suitable solvent should have both a high selectivity and a high capacity for the component to be separated. The results obtained for  $S_{ij}^{\infty}$  and  $k_j^{\infty}$ , were calculated using Equations 14 and 15, and the results are presented in Table 3.

**Table 3.** Selectivities  $S_{ij}^{\infty}$  and capacities  $k_j^{\infty}$ , at infinite dilution for different separation systems.

| selectivities/capacities            |            |            |             |             |             |             |             |            |
|-------------------------------------|------------|------------|-------------|-------------|-------------|-------------|-------------|------------|
| System                              | 60°C       | 70°C       | 80°C        | 90°C        | 100°C       | 110°C       | 120°C       | 130°C      |
| Octane/benzene                      | 33.23/0.39 | 30.48/0.38 | 27.30/0.38  | 26.04/0.38  | 24.68/0.38  | 21.86/0.38  | ---         | ---        |
| Cyclohexane/Benzene                 | 7.87/0.39  | 7.51/0.38  | 6.96/0.38   | 6.66/0.38   | 6.36/0.38   | 5.69/0.38   | ---         | ---        |
| Cyclohexane/thiophene               | 16.44/0.84 | 15.21/0.78 | 13.76/0.75  | 12.85/0.74  | 11.95/0.71  | 10.46/0.69  | ---         | ---        |
| Octane/pyridine                     | 67.88/0.79 | 62.38/0.79 | 55.68/0.78  | 52.88/0.77  | ---         | 44.37/0.76  | ---         | ---        |
| $\alpha$ - pinene/ $\beta$ - pinene | ---        | ---        | 1.34/0.03   | 1.38/0.03   | 1.35/0.03   | 1.32/0.04   | 1.31/0.04   | 1.33/0.04  |
| Limonene/Menthone                   | ---        | ---        | 9.50/0.31   | 10.13/0.33  | 10.76/0.35  | 13.90/0.45  | 14.84/0.38  | 14.38/0.35 |
| selectivities/capacities            |            |            |             |             |             |             |             |            |
| System                              | ---        | ---        | 140°C       | 145°C       | 150°C       | 155°C       | 160°C       | 165°C      |
| Limonene/Linalool                   | ---        | ---        | 170.15/5.26 | 148.74/4.64 | 123.36/3.79 | 129.82/3.72 | 118.85/3.32 | 98.57/2.76 |

The limonene/linalool separation is the easiest separation, and the system  $\alpha$ -pinene/ $\beta$ -pinene the most difficult. The result obtained with limonene/linalool is likely a result of the preferential interaction that the (hydrogen accepting) acetate anions can establish with the (hydrogen donating) hydroxyl group of the linalool. The results obtained for the system limonene/linalool were obtained in a different temperature range and using the first column because this IL suffers degradation at high temperatures or at lower temperatures with a long time of operation (Cao and Mu, 2014). The anion type plays the major role on the thermal stability of ILs, then the cation type, while cation modification has the least effect. The thermal stability of ILs increases with shorter chain length, greater substituent number, and replacing C<sub>2</sub>-H with a methyl group (Cao and Mu, 2014).

Unfortunately, the high retention time of linalool demanded high operation temperatures. Cao and Mu (2014) shows that the decomposition temperature for this IL is 489.15 K, value that was obtained by a TGA, being this temperature of onset. But for 10 hours of work, 1% of mass is lost at 385.95 K, which proved that the thermal stability of this IL was not guaranteed and showed least stable if compare with other ILs studied (Cao and Mu, 2014). The extrapolated values to room temperature (298.15 K) of the selectivity of limonene/linalool was 452.97 and 15.96 was the capacity.

Besides, the values of the selectivity and capacity of the systems octane/benzene, cyclohexane/benzene, cyclohexane/thiophene, were compared with three ILs presented in the literature. Those results were cited by Martins et al. (2015) and a comparison with the IL studied in this work is presented in Table 4.

**Table 4.** Comparison of selectivities  $S_{ij}^{\infty}$  and capacities  $k_j^{\infty}$ , at infinite dilution for different studies at 85°C.

| Ionic Liquid         |   |                |                     |                       |                                  |
|----------------------|---|----------------|---------------------|-----------------------|----------------------------------|
| Cation               | Anion   | Octane/benzene | Cyclohexane/benzene | Cyclohexane/thiophene | Reference                        |
| [C4mim] <sup>+</sup> | [OAc] <sup>-</sup>  | 27.30/0.38     | 6.96/0.38           | 13.76/0.75            | This work                        |
|                      | Cl <sup>-</sup>   | 73.32/0.22     | 12.13/0.22          | 26.75/0.49            | (Martins et al., 2016)           |
|                      | [CH <sub>3</sub> SO <sub>3</sub> ] <sup>-</sup>   | 55.50/0.32     | 11.43/0.32          | 20.41/0.58            | (Martins et al., 2016)           |
|                      | [(CH <sub>3</sub> ) <sub>2</sub> PO <sub>4</sub> ] <sup>-</sup>                                 | 20.58/0.43     | 5.28/0.43           | 9.88/0.80             | (Martins et al., 2016)           |
|                      | [(CH <sub>3</sub> (CH <sub>2</sub> ) <sub>3</sub> ) <sub>2</sub> PO <sub>4</sub> ] <sup>-</sup> | 7.20/1.17      | 3.06/1.17           |                       | (Ge et al., 2012)                |
|                      | [CF <sub>3</sub> SO <sub>3</sub> ] <sup>-</sup>   | 30.61/0.61     | 8.16/0.61           | 11.27/0.85            | (Domańska and Marciniak, 2008)   |
| [C8mim] <sup>+</sup> | Cl <sup>-</sup>   | 13.67/0.80     | 6.04/0.80           |                       | (David et al., 2003)             |
| [C2mim] <sup>+</sup> | [CH <sub>3</sub> SO <sub>3</sub> ] <sup>-</sup>   | 64.02/0.23     | 10.57b/0.23b        | 21.75/0.48            | (Domańska and Królikowski, 2012) |
|                      |   | 86.08/0.24     | 12.18/0.24          | 24.59/0.49            | (Moïse et al., 2011)             |
| [C1mim] <sup>+</sup> | [(CH <sub>3</sub> ) <sub>2</sub> PO <sub>4</sub> ] <sup>-</sup>                                 | 65.71/0.27     | 10.58/0.27          |                       | (Kato and Gmehling, 2004)        |
| [C2mim] <sup>+</sup> | [(CH <sub>3</sub> CH <sub>2</sub> ) <sub>2</sub> PO <sub>4</sub> ] <sup>-</sup>                 | 36.24/0.43     | 10.70/0.43          |                       | (Ge and Chen, 2011)              |

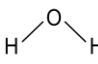
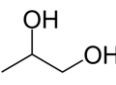
Analyzing Table 4, it is possible see that all the separations are harder using the IL of this work, than some others ILs showed in the table. The lowest values of selectivity are found for [C<sub>8</sub>mim]Cl and [C<sub>4</sub>mim][[(CH<sub>3</sub>(CH<sub>2</sub>)<sub>3</sub>)<sub>2</sub>PO<sub>4</sub>], both present a cation and an anion, respectively, with a longer alkyl chain making it difficult the separation.

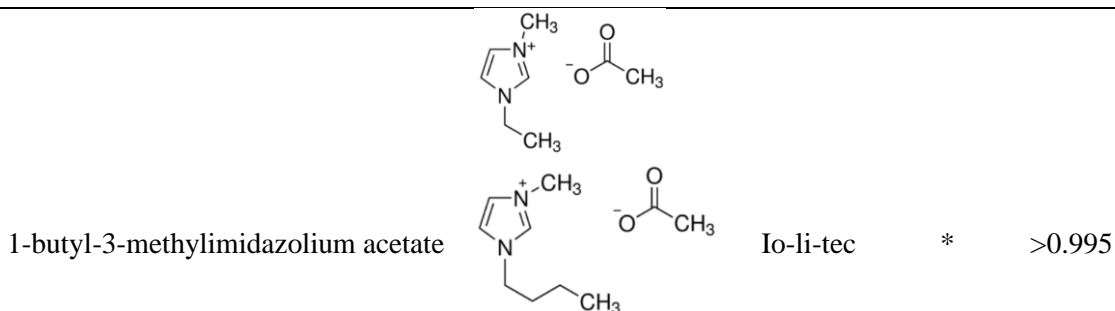
## Chapter 4. Experimental freezing point depression

### 4.1 Chemicals

The chemical structure, source, melting point temperature (TBP) and mass fraction purity indicated by the supplier are presented in Table 5.

**Table 5.** Name, structure, supplier, melting point (TMP) and purity of the investigated solutes.

|               | Chemicals                           | Structure   | Source             | TMP (K) | Mass fraction purity |
|---------------|-------------------------------------|---|--------------------|---------|----------------------|
|               | Water                               |  |                    | 373.15  |                      |
| Salts         | Calcium Chloride                    | CaCl <sub>2</sub>   | Honeywell<br>Fluka | 1045    | ≥0.995               |
|               | Sodium Chloride                     | NaCl  | Honeywell<br>Fluka | 1074    | ≥ 0.995              |
|               | 1,2-Propanediol                     |  | Aldrich            | 214.1   | >0.995               |
| Ionic liquids | 1-Ethyl-3-methylimidazolium acetate |   | Io-li-tec          | *       | >0.995               |



\* No melting point values were found for ionic liquids. The information available in the ILThermo database were the transition temperature glass-liquid.

Ultrapure water (resistivity of 18.2 MΩ.cm, free particles  $\geq 0.22 \mu\text{m}$  and total organic carbon  $< 5 \mu\text{d.dm}^{-3}$ ) was used to prepare the solutions.

#### 4.2 Experimental methodology

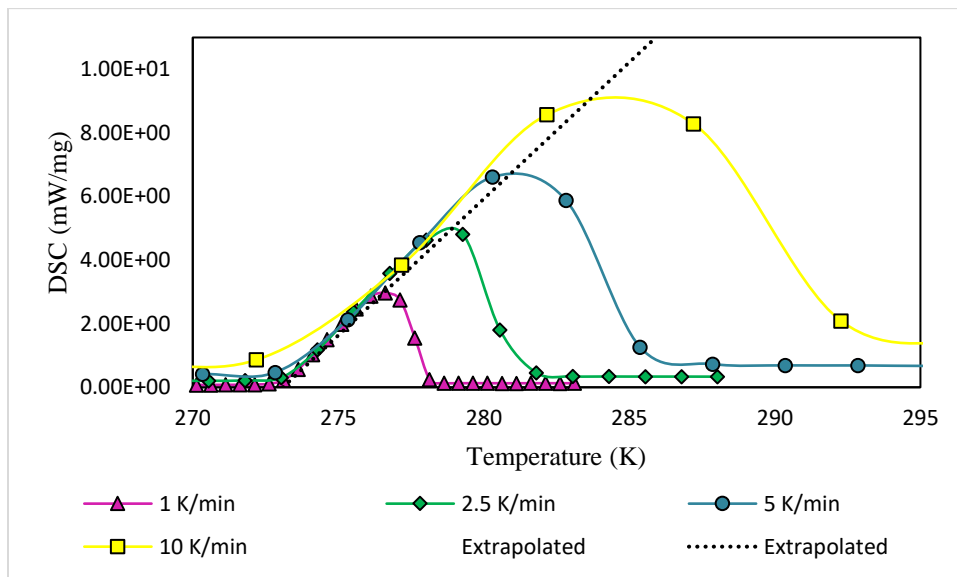
The freezing points properties were measured by Differential Scanning Calorimetry (DSC). The DSC 204 F1 Phoenix of Netzsch (Figure 13) had already been calibrated with benzoic acid, indium, caffeine, bismuth, 4-nitrofluorene, water, naphthalene, diphenylacetic acid, anthracene, tin, and zinc at the onset temperature, ensuring an accuracy within 1.53% in the temperature range from 0 °C to 420 °C. For temperatures below 0 °C, the cooling rate was 5 K·min<sup>-1</sup>, and the heating rates were 1 K·min<sup>-1</sup>, 5 K·min<sup>-1</sup>, and 10 K·min<sup>-1</sup> when the mass fraction was below 20%. For mass fractions above 20%, the heating rates were 1 K·min<sup>-1</sup>, 2.5 K·min<sup>-1</sup>, and 5 K·min<sup>-1</sup>, and the cooling rate was 5 K·min<sup>-1</sup>. The minimum temperature reached was approximately -80°C.



**Figure 13.** DSC used in this work.

All the samples were weighed by an analytical balance with an accuracy of  $\pm 0.1$  mg. The water contents in the calcium chloride dihydrate, 1,2-propanediol and ILs were measured by Karl Fischer titration and they were considered in the calculation of the compositions of the solutions. To check the use of DSC for freezing point depression studies, water and aqueous solutions of NaCl, CaCl<sub>2</sub>, 1,2-propanediol, 1-ethyl-3-methylimidazolium acetate, and finally, 1-butyl-3-methylimidazolium acetate were used. This selection aimed to test this methodology with salts, one organic liquid (1,2-propanediol) and then the ILs.

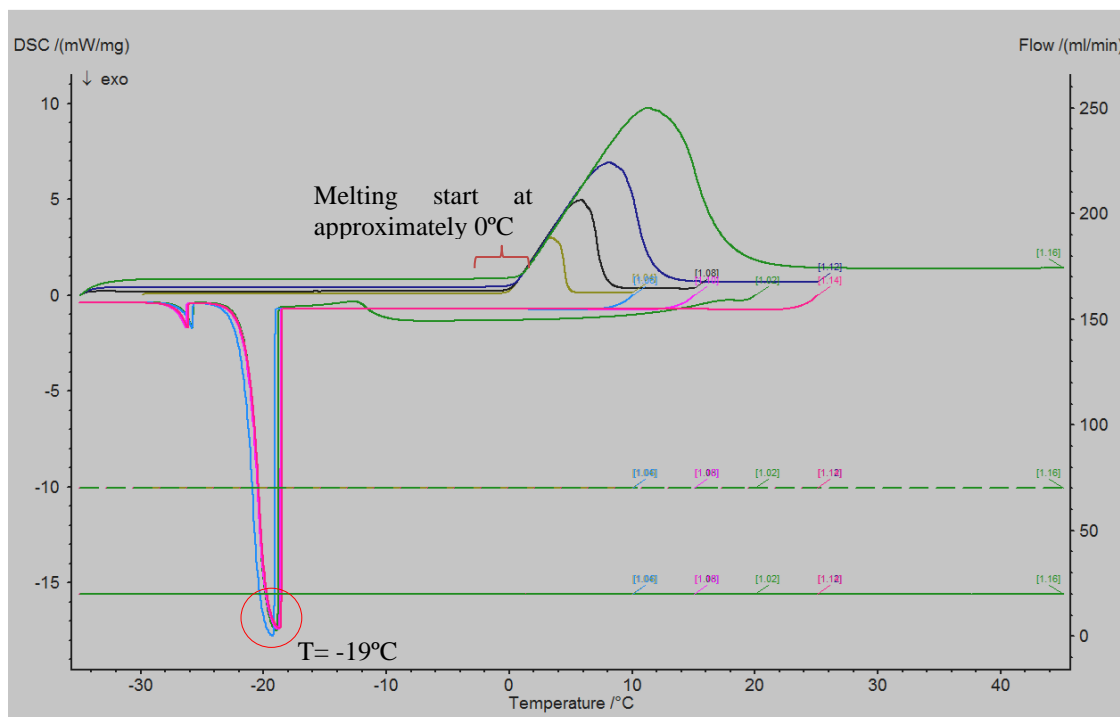
This test was done to verify the results showed by our equipment. As can be seen in Figure 14, in the thermogram of water obtained by DSC, the result extrapolated was very satisfactory with  $R^2 = 0.99874$ .



**Figure 14.** Thermogram of water extrapolated to 273.10 K.

It is possible to see in Figure 15 when the sample freezes, characterized by the peaks at approximately  $-19$  °C (the four times at 5 K/min), and started to melt close to  $0$  °C described by the peaks with positive temperatures, being the yellow line at 1 K/min to 10 K/min (green line).





**Figure 15.** Thermogram of water with different heating rates (1, 2.5, 5 and 10 K/min).

To the test of NaCl, an aqueous solution of 10% mass fraction was prepared and three independent samples were measured. The first and second samples were cooled with cooling rate of 1 K/min to a temperature of -50 °C, and held at that temperature for 3 min. Then the samples were heated to a temperature close to 20 °C with heating rate of 1 K/min. It was possible to observed that it was not necessary to cool until -50 °C because the eutectic point occurred around -21°C where there are ice and NaCl in solid state. In this way, it is possible some time savings and preservation of equipment. In the third run, the sample was cooled until -30 °C, this temperature was maintained for 3 min with the same cooling/heating rate, the sample was heated to 20 °C, held for 3 min and then the procedure was repeated to analyze if the methodology can be reproducible.

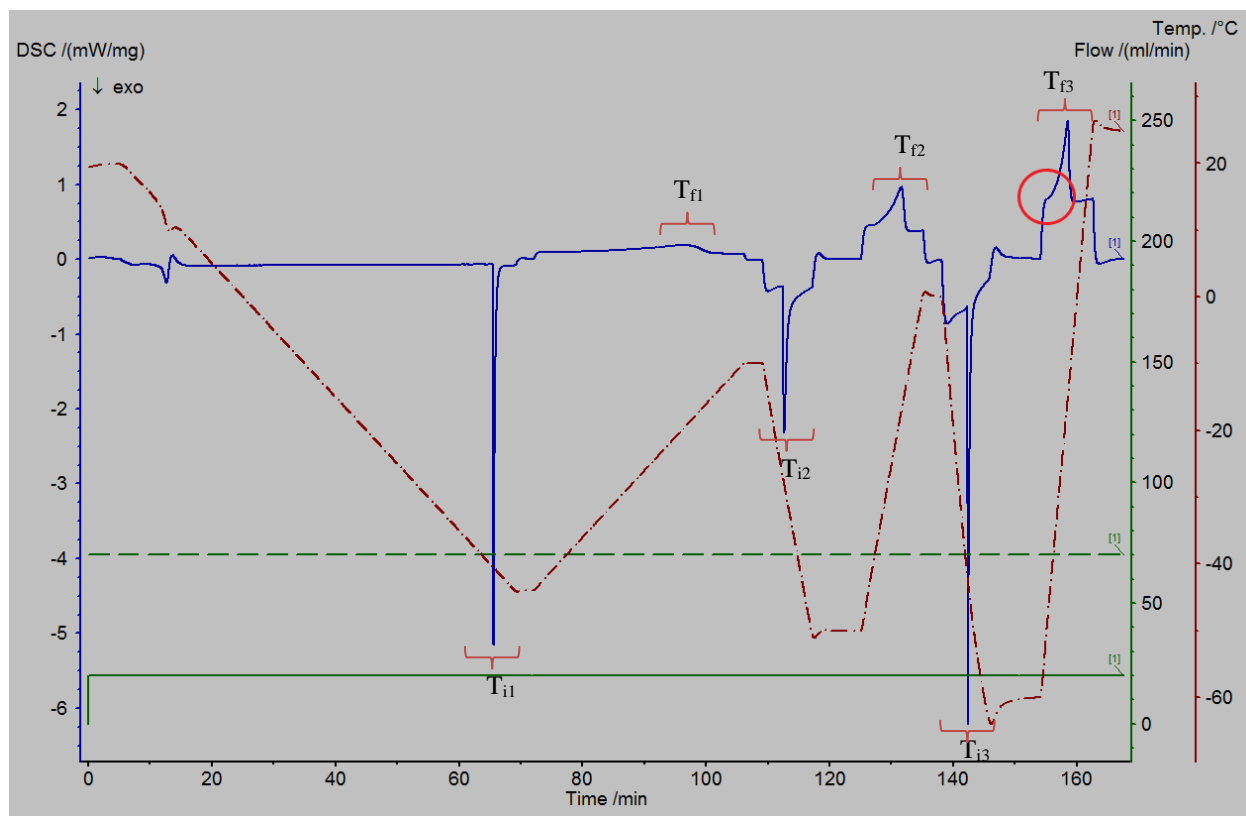
To analyze the freezing depression effect of CaCl<sub>2</sub>, a mother solution was prepared with concentration of 60% in mass, that was used to prepare all other concentrations, namely 5, 10, 15, 20, 25 or 30% in mass. The samples were prepared in bottles, from which a small amount was collected (8-17 mg) and added into an aluminum sample pan. The thermograms were acquired twice at all the selected concentrations. The values of the concentration and heating/cooling rates used in DSC runs are presented in Table 6:

**Table 6.** Freezing point data of calcium chloride aqueous solutions.

| Mass percentage | Freezing point first sample (°C) | Freezing point second sample (°C) | Cooling rate first sample (K/min) | Cooling rate second sample (K/min) | Heating rate first sample (K/min) | Heating rate second sample (K/min) |
|-----------------|----------------------------------|-----------------------------------|-----------------------------------|------------------------------------|-----------------------------------|------------------------------------|
| 4.99            | -2.52                            | -2.51                             | 1;5;10                            | 5                                  | 1;5;10                            | 1;5;10                             |
| 9.94            | -6.00                            | -6.28                             | 1;5;10                            | 5                                  | 1;5;10                            | 1;5;10                             |
| 14.59           | -11.03                           | -11.31                            | 1;5;10                            | 5                                  | 1;5;10                            | 1;5;10                             |
| 19.88           | -20.70                           | -19.47                            | 1;5;10                            | 5                                  | 1;5;10                            | 1;2.5;5                            |
| 24.73           | -31.30                           | -30.72                            | 1;5;10                            | 5                                  | 1;5;10                            | 1;2.5;5                            |
| 29.97           | -52.44                           | -52.63                            | 1;5;10                            | 5                                  | 1;5;10                            | 1;2.5;5                            |

The difference between cooling rates of first and second samples, were made to observe if after freeze and melt, the sample would have the same behavior of cooling process showed in thermogram, once that was no stirrer on the sample, and then we wanted observe if the sample would freeze more easily.

The differences in heating rates between the samples with concentration above 20% mass fraction were defined because when the concentration increases, the melting point peak at 10 K/min rate in the thermogram was not clear to determine the start of fusion, as can be seen in Figure 18 (red circle).



**Figure 16.** Thermogram of 24.73% mass fraction of  $\text{CaCl}_2$ .

A peak begins at  $T_{i1}$  (first deviation from the baseline), and merges into the baseline at  $T_{f1}$ . In the region with the red circle, it is possible to see that is difficult to establish where  $T_f$  starts, so to guarantee the results with the minimum error, above 20% of mass fraction, the better heating rates were 1; 2.5 and 5 K/min.

Similarly to  $\text{CaCl}_2$ , two mother solutions were prepared with mass percentage of 60% of 1,2-propanediol. One of them was used to dilute to the desired concentrations; 5, 7, 10, 20, 30, 40, and 50% in mass, while the second solution was used to prepare the samples with 10; 30 and 40% in mass to compare the results between samples.

The value of concentration and heating/cooling rates used in DSC, and values of freezing point are presented below:

**Table 7.** Freezing point data of 1,2-propanediol aqueous solutions.

| Mass percentage<br>1 <sup>st</sup> sample | Mass percentage<br>2 <sup>nd</sup> sample | Freezing point first<br>sample (°C) | Freezing point<br>second<br>sample(°C) | Cooling rate<br>(K/min) | Heating rate<br>(K/min) |
|---|---|-------------------------------------|--|-------------------------|-------------------------|
| 4.98                                      | ---                                       | -1.33                               | ---                                    | 5                       | 1;5;10                  |

|       |       |        |        |   |         |
|-------|-------|--------|--------|---|---------|
| 7.01  | ---   | -1.98  | ---    | 5 | 1;5;10  |
| 10.88 | 10.80 | -3.14  | -3.10  | 5 | 1;5;10  |
| 19.21 | ---   | -6.70  | ---    | 5 | 1;2.5;5 |
| 29.94 | 30.75 | -13.24 | -13.88 | 5 | 1;2.5;5 |
| 40.18 | 43.25 | -21.73 | -24.81 | 5 | 1;2.5;5 |
| 50.19 | ---   | -33.32 | ---    | 5 | 1;2.5;5 |

In the next sections the results obtained in this work will be compared with results found in the literature.

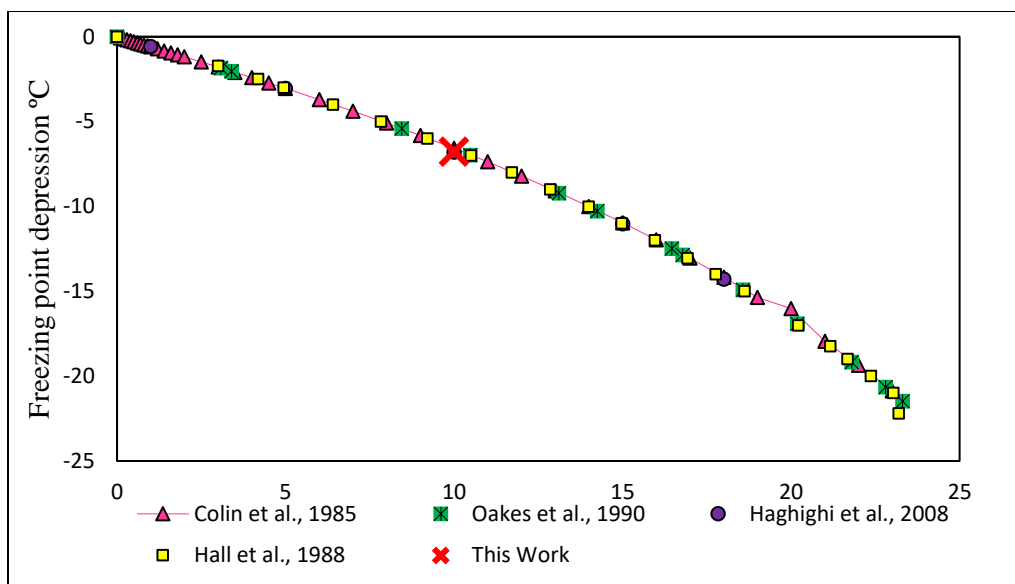
### 4.3 Aqueous solutions of NaCl

Table 8 shows a summary of the freezing point data of aqueous solutions of sodium chloride found in the literature.

**Table 8.** Freezing point data of sodium chloride aqueous solutions found in literature.

| Mass percentage | Temperature range/°C | Number of data points | Reference             |
|-----------------|----------------------|-----------------------|-----------------------|
| 1 to 18         | -0.58 to -14.29      | 5                     | Haghighi et al., 2008 |
| 0.1 to 24       | -0.06 to -20.86      | Correlation           | Colin et al., 1985    |
| 0 to 23.31      | 0 to -25             | 14                    | Oakes et al., 1990    |
| 0 to 23.2       | 0 to -22.1           | 22                    | Hall et al., 1988     |

Figure 16 compares the results obtained in this work with the literature whose references are presented in Table 8. It is easy to realize that our methodology gives a value in high agreement with the literature. All methodologies used, were other than DSC. The methodology used by Haghighi et al. (2008) was described previously in section 2.2.2. Colin et al. (1985) used the weighted least-squares method. The methodology used by Oakes et al. (1990) was a modification used by (Hall et al., 1988) that consist in cooling the water-salt solution at 3 °C below its freezing point, and then pure H<sub>2</sub>O ice will precipitate from the solution. With continued cooling additional, ice will precipitate causing the total salinity of the liquid phase in equilibrium with the ice.



**Figure 17.** Freezing point depression as a function of NaCl weight percentage, comparing the results obtained in this work with literature data.

In Appendix B1, B2 and B2 there are thermograms that shows that at  $-21\text{ }^{\circ}\text{C}$  there is a peak that represents the solidus line transition, and at around  $-6.7\text{ }^{\circ}\text{C}$  another peak representing the liquidus line temperature. Because of eutectic point showed at  $-21\text{ }^{\circ}\text{C}$ , it was necessary to change the testing salt. If NaCl was kept, the peak of ice transition and the peak of eutectic would eventually overlap, and the procedure could not be tested conveniently. Another relevant question is, to test ILs, it will be necessary to reach lower temperatures. So, a known system with temperatures below that of NaCl is needed to compare with the data obtained in DSC at low temperatures. The chosen salt was  $\text{CaCl}_2$ .

#### 4.4 Aqueous solutions of $\text{CaCl}_2$

It was made a comparison between methodologies already studied (Table 9) and the methodology of DSC to analyze the freezing point depression of water with different mass fraction of  $\text{CaCl}_2$ .

**Table 9.** Freezing point data of calcium chloride aqueous solutions found in literature.

| Mass fraction (%) | Temperature range/°C | Number of data points | Reference              |
|-------------------|----------------------|-----------------------|------------------------|
| 5.76 to 32.43     | -3.48 to -51.00      | 18                    | Roddbush, 1918         |
| 0.61 to 13.90     | -0.14 to -3.95       | 10                    | Gibbard and Fong, 1975 |
| 0 to 30.59        | 0 to -51.20          | 60                    | Oakes et al., 1990     |
| 0.50 to 32        | 0 to -49.70          | Correlation           | NIST database*         |

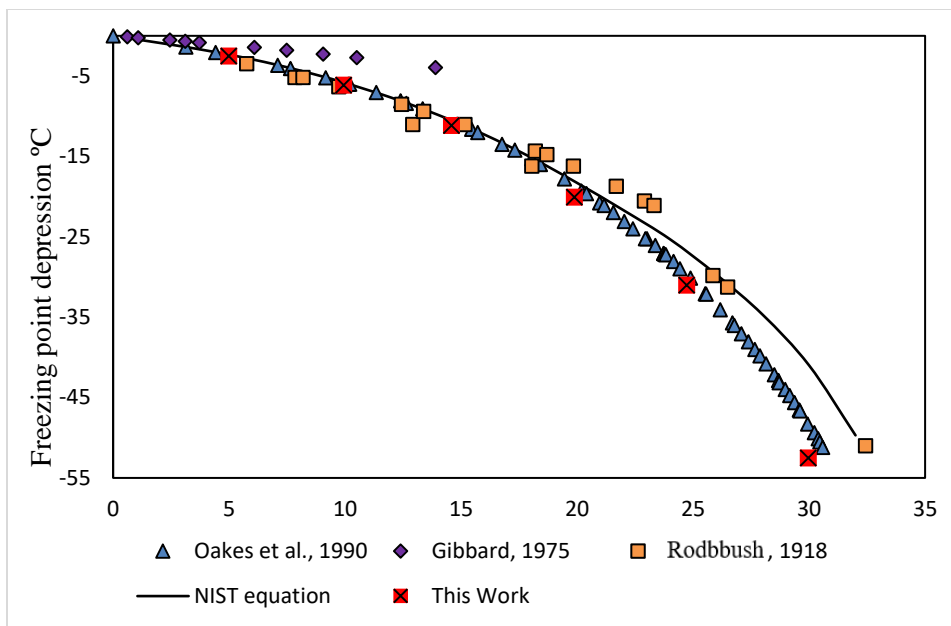
\*NIST – National Institute of Standards Technology

Roddbush (1918) used two tubes, one tube contained ice and water, used as a standard temperature bath. The other tube contained the mixture of ice and calcium chloride, containing a stirrer. When the temperature ceased falling and began to rise slowly a pipet was plunged into the solution through a hole in the stopper and a sample quickly drawn off and transferred to a stoppered flask for analysis, care being taken to prevent dilution of the solution by condensation of moisture from the air. The solutions of calcium were analyzed by precipitating the chlorine as silver chloride to measure the composition.

Gibbard and Fong (1975) followed a methodology similar to Roddbush (1918), using also two tubes, one with ice and water and the other with the mixture. Samples were removed with a syringe and warmed to room temperature in sealed bottles before they are weighed for gravimetric chloride analysis. Solution removed for analysis is replaced by cold water. In this way, a series of progressively more dilute solutions was studied (Gibbard and Fong, 1975).

Oakes et al. (1990) used the methodology described by Hall et al. (1988) to ice liquidus of  $\text{CaCl}_2$ . Simply stated, a low water-salt solution is cooled 3 °C below its freezing point, pure  $\text{H}_2\text{O}$  ice will precipitate from the solution. With continued cooling additional, ice will precipitate causing the total salinity of the liquid phase in equilibrium with the ice.

Figure 17 shows the comparison between this work and literature data. It is interesting to observe that our results are similar to those obtained by Oakes et al. (1990), Roddbush (1918) and the NIST correlation. However, our results differ from the results obtained by Gibbard and Fong (1975), and their results differ from the results presented by Roddbush (1918) being that the methodology used was very similar. Maybe the difference between results of Gibbard and Fong (1975) and Roddbush (1918) is because in work of Gibbard and Fong (1975) they used a term “equivalent molality” being the concentration equivalent, however they do not make it clear what type of consideration was made to obtain values of equivalent molality.



**Figure 18.** Freezing point depression as a function of  $\text{CaCl}_2$  weight percentage, comparing the results obtained in this work with literature data.

#### 4.5 Aqueous solutions of 1,2-propanediol

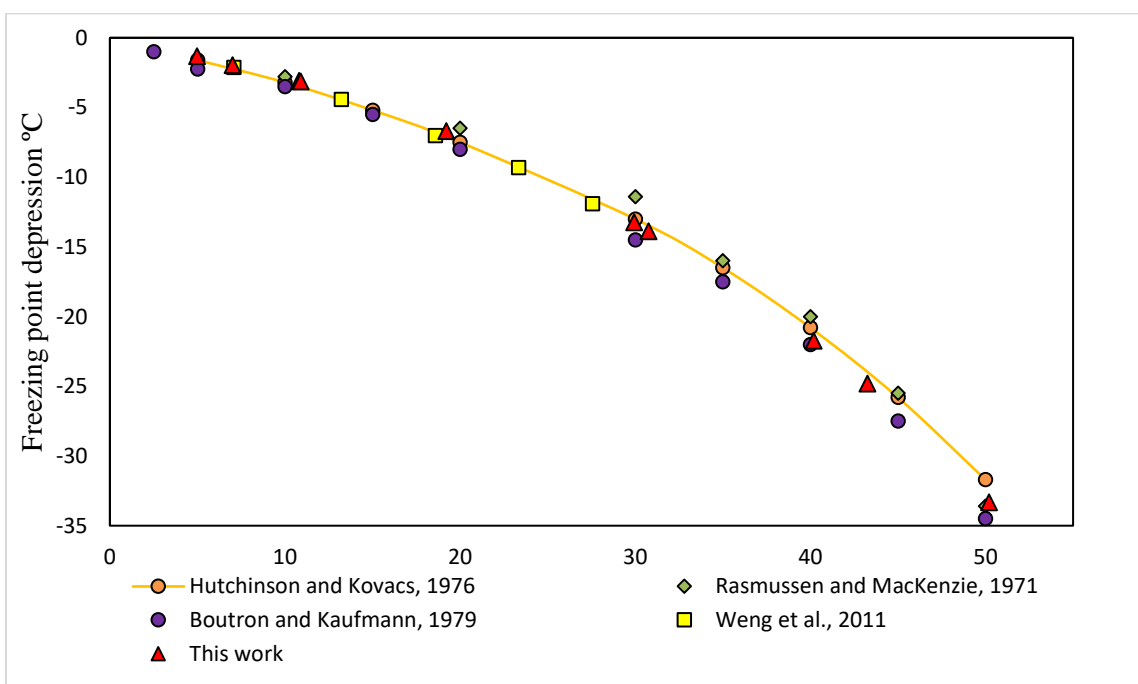
It was made a comparison between methodologies already studied by previous works and the methodology of DSC to analyze the freezing point depression of water at different mass fraction of 1,2-propanediol.

**Table 10.** Freezing point data of 1,2-propanediol aqueous solutions found in literature.

| Mass percentage | Temperature range/°C | Number of data points | Reference                     |
|-----------------|----------------------|-----------------------|-------------------------------|
| 5 to 50         | -1.60 to -31.70      | correlation           | Hutchinson and Kovacs, 1976   |
| 1 to 50         | -2.80 to -33.60      | 7                     | Rasmussen and MacKenzie, 1971 |
| 7 to 27         | -2.13 to -11.91      | 5                     | Weng et al., 2011             |
| 2 to 50         | -1.00 to -34.50      | 10                    | Boutron and Kaufmann, 1979    |

Weng et al. (2011) and Boutron and Kaufmann, (1979) used the DSC to measure the freezing point of propylene glycol aqueous solutions, allowing to compare directly to the results found in this work. Rasmussen and MacKenzie, (1971) used the methodology of differential thermal analysis (DTA), while Hutchinson and Kovacs, (1976) used an equation already proposed by Kovacs,

(1966) analyzed in terms of retardation kinetics. It is a phenomenological theory involving a single retardation time, assuming that molecular mobility is controlled essentially by the actual free volume, or configurational entropy of the glassy specimen. Through Figure 19, it is possible compare the results obtained in literature and this work, highlighting that Weng et al. (2011) and Boutron and Kaufmann, (1979) used the same methodology as this work and the behavior was the same. Rasmussen and MacKenzie, (1971) used a similar methodology with DSC, but the DTA measures the temperature difference during heating or cooling while DSC measures the heat absorbed or liberated during heating or cooling. For both DTA and DSC, the first measured signal is the temperature difference between a sample and the reference, in  $\mu\text{V}$ . For DSC, this temperature difference can be converted into a heat flux, in  $\text{mW}$ , by means of an appropriate calibration. This possibility does not exist in a DTA instrument.



**Figure 19.** Freezing point depression as a function of 1,2-propanediol weight fraction, comparing the results obtained in this work with literature data.

The fact that the methodologies found in the literature present the same results, shows that the DSC can be used to obtain the freezing point depression, not only for organic liquids but also for salts as shown previously. This is a good information that is possible to move on to the analysis of solid-liquid equilibria of 1-ethyl-3-methylimidazolium acetate and 1-butyl-3-methylimidazolium acetate aqueous solutions.

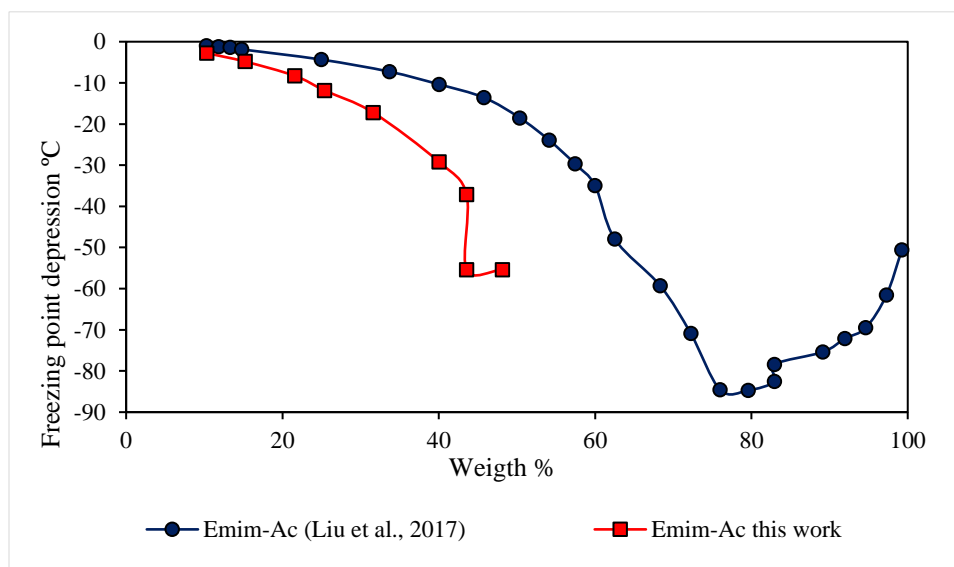


Of course, this equipment has some limitations such as inaccuracy in determining peak areas due to baseline changes during a transition if the cooling or heating rate are fast. Another limitation (in this case) is that temperature is limited to approximately  $-80^{\circ}\text{C}$ . However, its advantages outweigh its disadvantages, e.g. it is necessary only small quantities of sample. The sensibility of measurement of heat of transition is accurate, and using this model, we can also give a physical meaning to the thermogram shape and we can easily detect the end point of the phase transformation (Kousksou et al., 2007).

Among these and other advantages, the DSC as seen, can be used to determine the phase diagram of salts and organic liquids as 1,2-propanediol. In order to evaluate the possibility of separating a known binary mixture by using the crystallization method having the accurate solid-liquid equilibrium (SLE) data for the system is crucial (Noshadi and Sadeghi, 2018). Now we will investigate if this technique works well with ionic liquids.

#### 4.6 Aqueous solutions of 1-ethyl-3-methylimidazolium acetate

A comparison was made between only one previous work and the methodology of DSC to analyze the freezing point depression of water at different mass fraction of 1-ethyl-3-methylimidazolium acetate. Figure 20 shows the difference between our results and the results presented by Liu et al. (2017). Despite being different methodologies, it has no data to confirm the quality of the results, once there is only this work to compare, so it is necessary to apply alternative techniques and obtain more data from independent sources.



**Figure 20.** Freezing point depression as a function of EmimAc mass fraction, comparing the results obtained in this work with literature data.

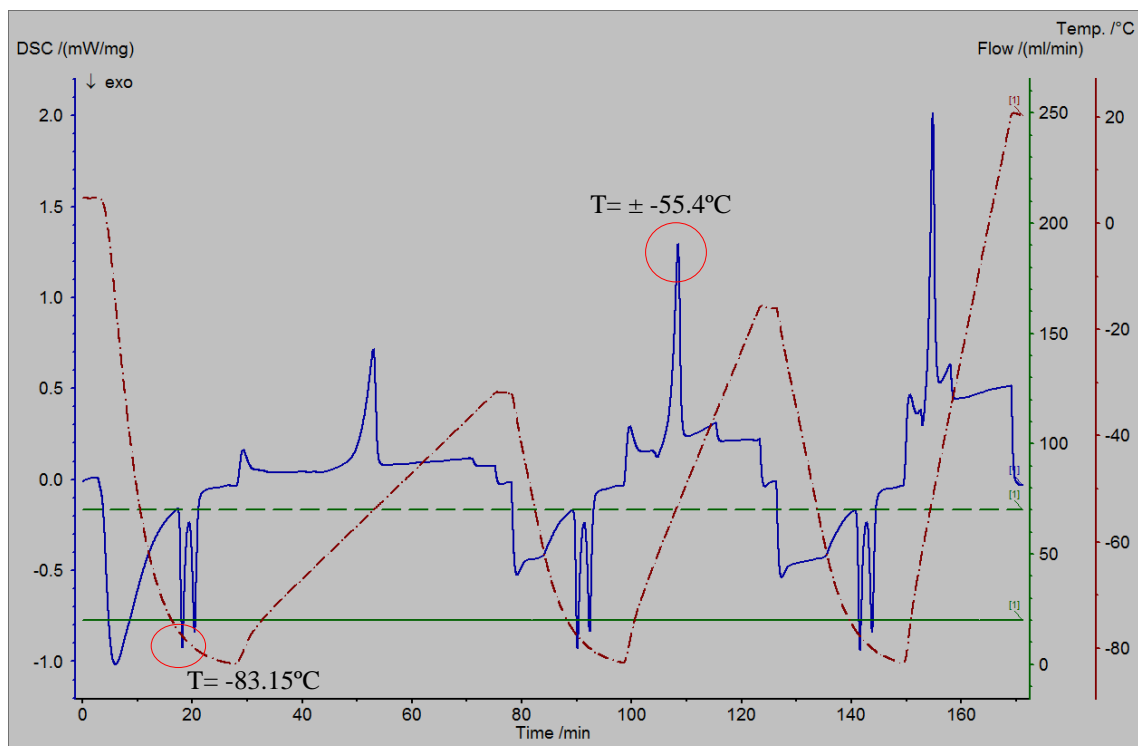
The way of obtaining our results is extrapolating the curves provided by DSC with different rates, until zero heating rate, while Liu et al. (2017) under-cooled the IL+H<sub>2</sub>O solutions by liquid nitrogen. Then they were held and stirred at room temperature until all crystals had disappeared. At this point the freezing points were determined.

Table 11 shows the values obtained with different mass fractions and the program to heat and cool each sample.

**Table 11.** Freezing point data of EmimAc aqueous solutions.

| Mass percentage<br>1 <sup>st</sup> sample | Mass percentage<br>2 <sup>nd</sup> sample | Freezing point first<br>sample<br>(°C) | Freezing point second<br>sample(°C) | Cooling rate<br>(K/min) | Heating rate<br>(K/min) |
|---|---|--|-------------------------------------|-------------------------|-------------------------|
| 10.51                                     | 10.50                                     | -2.79                                  | -2.83                               | 5                       | 1;5;10                  |
| 15.46                                     | ---                                       | -4.83                                  | ---                                 | 5                       | 1;5;10                  |
| 21.94                                     | ---                                       | -8.30                                  | -3.10                               | 5                       | 1;5;10                  |
| 25.81                                     | ---                                       | -11.84                                 | ---                                 | 5                       | 1;2.5;5                 |
| 32.15                                     | 31.68                                     | -17.23                                 | -16.42                              | 5                       | 1;2.5;5                 |
| 40.02                                     | 43.56                                     | -29.20                                 | -37.17                              | 5                       | 1;2.5;5                 |
| 48.16                                     | ---                                       | -55.43                                 | ---                                 | 5                       | 1;2.5;5                 |

One different behavior was obtained at 43.56% of mass fraction of EmimAc (Figure 21), when a second peak was observed. It is possible that it is the eutectic point peak that crystallized near to -83.15°C and melted at -55.4°C (extrapolated). The temperature program is indicated by the dashed line.



**Figure 21.** Thermogram of 43.56% mass fraction of EmimAc. The cooling rate used was 5 K/min and the heating rates used were 1, 2.5 and 5 K/min.

The eutectic peak also showed a different value compared with the literature data. While in this work the value was  $-55.4\text{ }^{\circ}\text{C}$ , in the work of Liu et al. (2017), the eutectic point showed the value of  $-83.15\text{ }^{\circ}\text{C}$ . It means that there is no relation between results, because the value considered eutectic point obtained by this work ( $-55\text{ }^{\circ}\text{C}$ ), is very close of value obtained as melting point of EmimAc ( $-50\text{ }^{\circ}\text{C}$ ) by Liu et al. (2017). To have a value for the melting point so close to the value obtained for the eutectic point, it hardly never happens, which reinforces the need for new measurement methods to obtain the SLE of binary system water/EmimAc.

Some remarks can be made in work of Liu et al. (2017). The first observation is that they calibrated the equipment with different concentrations of NaCl, but the temperatures reached during the experiments were much lower than the crystallization temperature of NaCl aqueous solutions, which would imply the need to calibrate with solutions that presented similar temperatures to those reached.

The second observation is that they compared their results (using ILs) with results presented in another works, using different compounds (two salts,  $\text{MgCl}_2$  and  $\text{MgSO}_4$ ) and different

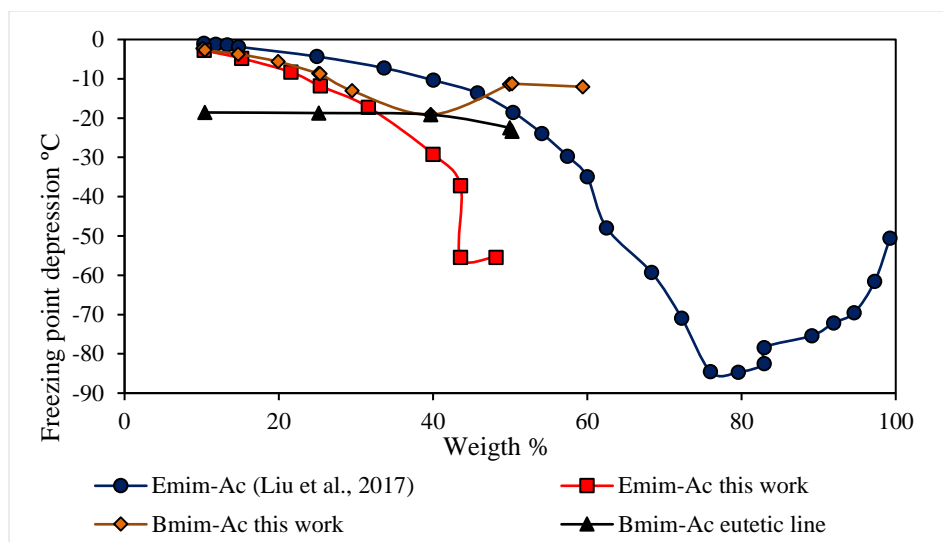
methodologies. Liu et al. (2017) should have used the same two salts and compared with the values in the literature.

In relation to freezing depression point, there is a study about the magnitude the hydrogen-bonding interaction between cation and anion of pure EmimAc and then extremely diluted in water (Chen et al., 2015). They concluded that there is not fully dissociation of EmimAc in water (0.5 mol%) because of ion pairing, through weak van der Waals force. In other words, when there is no complete dissociation, the freezing depression tends to be less if compared with complete dissociation.

#### **4.7 Aqueous solutions of 1-butyl-3-methylimidazolium acetate**

The interest in the properties of 1-butyl-3-methylimidazolium acetate (BmimAc)/water system is motivated by the fact that this ionic liquids can be applied as solvents for liquid–liquid extraction processes (Marekha et al., 2015).

It is likely a result of the preferential interaction that the (hydrogen accepting) acetate anions can establish with the (hydrogen donating) hydroxyl group of the solvents (Lago et al., 2014). The comparison between the SLE diagram for aqueous solutions of EmimAc and BmimAc is shown in Figure 22, that shows the difference between EmimAc and BmimAc diluted in water. Both ILs have the same anion that is very hygroscopic if compared to other ILs. This tendency was explained by the ability of water to form strong hydrogen bonds with the anions than with cation of the ILs. However, BmimAc is more apolar than EmimAc due to a longer alkyl chain than in the EmimAc, which confers a decrease (even if small) in the polarity of the BmimAc. The water that is strongly polar, interacts better with the more polar elements, in this case, EmimAc. So, the activity coefficient of BmimAc is higher than that of EmimAc. Therefore following Equation 6, to obtain the same freezing point depression, it is required more mass of BmimAc than EmimAc, as can be observed in Figure 22, when approximately 30% of EmimAc causes the freezing point depression to approximately -20 °C when to obtained the same effect, it was necessary approximately 40% in mass of BmimAc.



**Figure 22.** Comparison of freezing point depression for aqueous solutions of EmimAc or BmimAc.

Until analyzing Figure 22, the values represented by the triangular marker shows an indicative of eutectic value at approximately -20 °C at 39% mass fraction of BmimAc. It was tested four times and the results achieved were similar. The values are presented in Table 12.

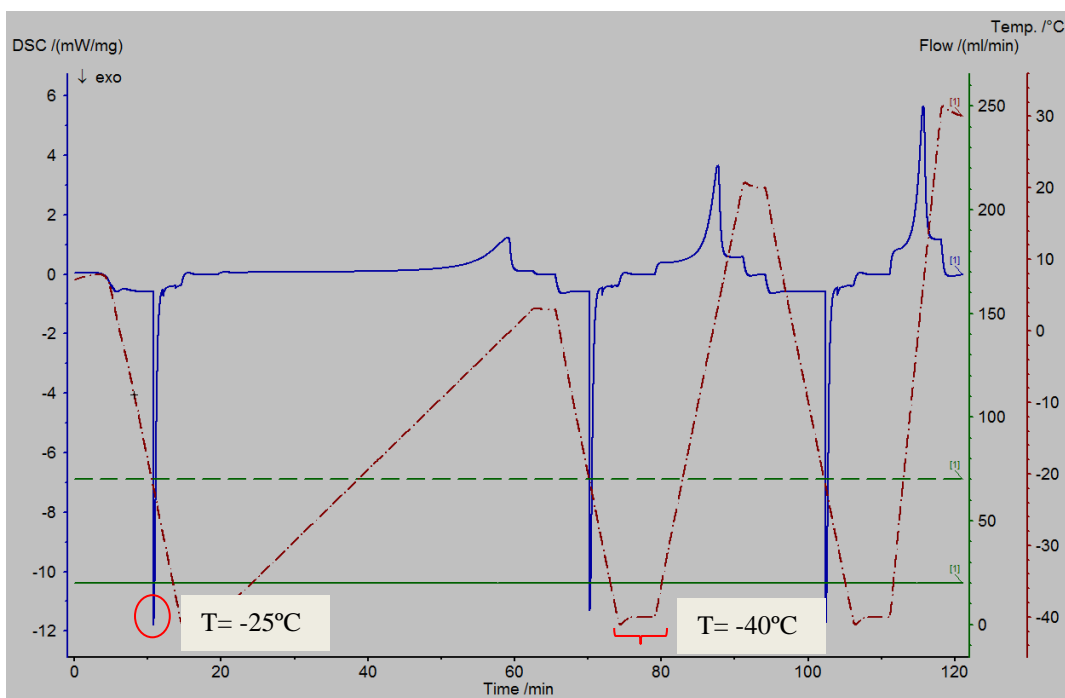
**Table 12.** Freezing point data of BmimAc aqueous solutions.

| Mass percentage 1 <sup>st</sup> sample | Mass percentage 2 <sup>nd</sup> sample | Freezing point first sample (°C) | Freezing point second sample(°C) | Cooling rate (K/min) | Heating rate (K/min) |
|--|--|----------------------------------|----------------------------------|----------------------|----------------------|
| 10.18                                  | 10.43                                  | -2.31                            | -18.58*                          | 5                    | 1;5;10               |
| 14.74                                  | 10.43                                  | -3.73                            | -2.70                            | 5                    | 1;5;10               |
| 19.919                                 | 25.20                                  | -5.64                            | -8.68                            | 5                    | 1;5;10               |
| 25.20                                  | 25.20                                  | -8.66                            | -18.72*                          | 5                    | 1;2.5;5              |
| 29.52                                  | ---                                    | -13.05                           | ---                              | 5                    | 1;2.5;5              |
| 39.74                                  | 50.26                                  | -19.14                           | -23.35*                          | 5                    | 1;2.5;5              |
| 49.95                                  | 50.26                                  | -22.48*                          | -11.26                           | 5                    | 1;2.5;5              |
| 49.95                                  | 59.42                                  | -11.42                           | -12.03                           | 5                    | 1;2.5;5              |

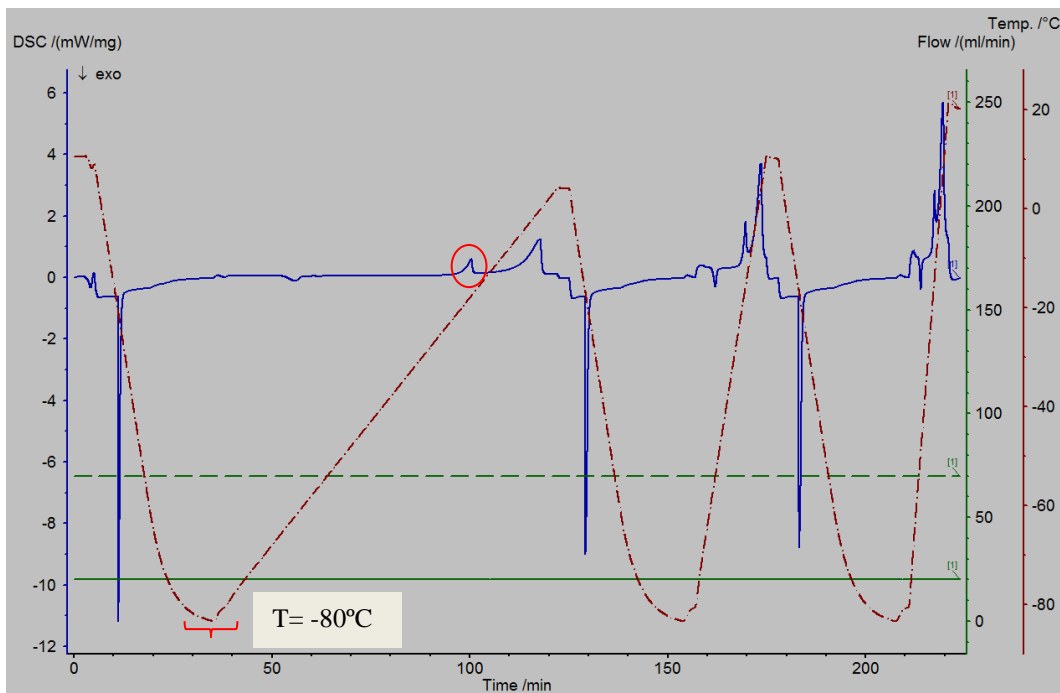
\*Temperature obtained to possible eutectic point.

The tests that was made to obtain the eutectic peak of BmimAc was achieved easier than the EmimAc tests. Figure 23 shows the first test of BmimAc 10% mass percentage. The temperature lowered to -40 °C to stabilize the baseline, once the water in this condition, cools at approximately -25 °C. The Figure 24 shows the same test of Figure 23, but with temperatures below -80 °C. In

this test is possible to see the eutectic peak (indicated by the red circle). Both tests had similar concentration, with different temperature program. This difference between temperature programs allows to obtain eutectic peak (circle) in the second test. That is, if we had lowered more the temperature when the sample of EmimAc was freezing, perhaps we also would get the formation of eutectic peak of this ionic liquid.



**Figure 23.** Thermogram of 10% mass of BmimAc.



**Figure 24.** Thermogram of 10% mass of BmimAc with eutectic point.

Analyzing the structure of BmimAc,  $C_{\text{alkyl}}$  (that is carbon present in the chain) of the cation shows a different tendency compared to that of cation ring  $C_{\text{ring}}$  (carbon present in the ring).  $C_{\text{alkyl}}\text{H}$  decreases its intensity (opposite to cation ring H) but shifts to a higher wavenumber (the same with cation ring H). It means that the interactions of  $C_{\text{alkyl}}\text{H}/\text{anion}$  and  $C_{\text{ring}}\text{H}/\text{anion}$  are different after introducing the water. In this case, it is not favorable for  $C_{\text{alkyl}}\text{H}$  to form hydrogen bonds with an anion, whereas  $C_{\text{alkyl}}\text{H}$  could form a nonpolar domain by a weak van der Waals force, which could be reduced by the expansion of the nonpolar domain after absorbing water (Chen et al., 2014). This behavior resembles EmimAc, which does not fully dissociate when diluted in water, but to BmimAc due to the lower polarity of the chain, the dissociation occur less than EmimAc, what explain the eutectic point to be less ( $-20^{\circ}\text{C}$ ) than eutectic point of EmimAc ( $-55^{\circ}\text{C}$ ), that is, it is easier to separate BmimAc/ water, than EmimAc/water.

## Chapter 5. Conclusions and future work

In this work, the activity coefficients at infinite dilution in 1-butyl-3-methylimidazolium acetate was measured by (gas + liquid) chromatography techniques for 44 organic solutes and water, at six different temperatures and three different temperatures for alcohols. Thermodynamic functions at infinite dilution and (gas + liquid) partition coefficients were analyzed and it was concluded that the hydrogen bonding between organic solutes and the acetate anion plays a significant role on the interaction of the ILs with organic solutes and determines the enthalpic behavior of the binary mixtures. The ability of the IL to act as entrainers in important separations was evaluated. Despite the lower capacities obtained for the different separation processes studied, the selectivities achieved were quite high and, this IL could be used as an alternative separating agent for limonene/linalool system. As suggestion, the values of the activity coefficients at infinite solution of 1-butyl-3-methylimidazolium acetate could be measured at 135 °C to compare with the values presented in the work of Martins et al. (2015) that were calculated by simulation with COSMO-RS.

The DSC methodology to analyze the freezing point of aqueous solutions of ILs was used to analyze a method of recovery of IL after being used in liquid-liquid extraction. The values of the aqueous solutions of NaCl, CaCl<sub>2</sub> and 1,2-propanediol agreed with literature.

For comparison, the freezing point data of aqueous solutions of 1-ethyl-3-methylimidazolium did not agree with literature. It was possible to obtain one value of possible eutectic point that also



disagrees with the literature value. Other tests must be made to prove and compare the results with this work. Relatively to 1-butyl-3-methylimidazolium acetate systems, no results were found in the literature. However, it was possible compare with the 1-ethyl-3-methylimidazolium acetate that is more polar than 1-butyl-3-methylimidazolium acetate and because of that, its interaction with water is higher. It means that is easier to separate water/BmimAc, than water/EmimAc. Further tests need to be done with the two pure ionic liquids in order to try to obtain their melting point.

Finally, the importance of this work is due to the fact that the methodology of activity coefficient at infinity dilution by gas chromatography showed that the separation of limonene/linalool is possible and applicable in industries to application of limonene in biodegradable solvents and application of linalool in perfumery industries and the advantage is that possible recovery the ionic liquid used through freezing point depression of water/1-butyl-3-methylimidazolium acetate once that was possible freeze water. So, the costs to obtain the IL will be minimized and we would have the use of an environmentally friendly solvent.

## References

- Almeida, H. F. D., Passos, H., Lopes-Da-Silva, J. A., Fernandes, A. M., Freire, M. G., & Coutinho, J. A. P. (2012). Thermophysical properties of five acetate-based ionic liquids. *Journal of Chemical and Engineering Data*, 57(11), 3005–3013.
- Anastas, P., & Eghbali, N. (2010). Green chemistry : principles and practice. *Chemical Society Reviews*, 39, 301–312.
- Arce, A., Marchiaro, A., Rodríguez, O., & Soto, A. (2006). Essential oil terpenless by extraction using organic solvents or ionic liquids. *Aiche J.*, 52(6), 2089–2097.
- Arce, A., Pobudkowska, A., Rodríguez, O., & Soto, A. (2007). Citrus essential oil terpenless by extraction using 1-ethyl-3-methylimidazolium ethylsulfate ionic liquid: Effect of the temperature. *Chemical Engineering Journal*, 133(1–3), 213–218.
- Arshad, M. W., Fosbøl, P. L., Von Solms, N., & Thomsen, K. (2013). Freezing point depressions of phase change CO<sub>2</sub> solvents. *Journal of Chemical and Engineering Data*, 58(7), 1918–1926.
- Boutron, P., & Kaufmann, A. (1979). Stability of the amorphous state in the system water-1,2-Propanediol. *Cryobiology*, 16(6), 557–568.
- Cao, Y., & Mu, T. (2014). Comprehensive investigation on the thermal stability of 66 ionic liquids by thermogravimetric analysis. *Industrial and Engineering Chemistry Research*, 53(20), 8651–8664.
- Chen, Y., Cao, Y., Yan, C., Zhang, Y., & Mu, T. (2014). The dynamic process of atmospheric water sorption in [BMIM][Ac]: Quantifying bulk versus surface sorption and utilizing atmospheric water as a structure probe. *Journal of Physical Chemistry B*, 118(24), 6896–6907.
- Chen, Y., Li, S., Xue, Z., Hao, M., & Mu, T. (2015). Quantifying the hydrogen-bonding interaction between cation and anion of pure [EMIM][Ac] and evidencing the ion pairs existence in its extremely diluted water solution: Via <sup>13</sup>C, <sup>1</sup>H, <sup>15</sup>N and 2D NMR. *Journal of Molecular Structure*, 1079, 120–129.
- Clas, S., Dalton, C. R., & Hancock, B. C. (1999). Differential scanning calorimetry: applications in drug development. *Research Focus - Reviews*, 2(8), 311–320.
- Colin, E., Clarke, W., & Glew, D. N. (1985). Evaluation of the thermodynamic functions for aqueous sodium chloride from equilibrium and calorimetric measurements below 154 ° C. *Physical and Chemical Reference*, 14(1985), 489–610.
- Crowhurst, L., Mawdsley, P. R., Perez-arlandis, J. M., Salter, P. A., & Welton, T. (2003). Solvent–solute interactions in ionic liquids. *The Owner Societies*, 5, 2790–2794.
- Cruickshank, A. J. B., Gainey, B. W., Hicks, C. P., Letcher, T. M., Moody, R. W., & Young, C. L. (1967). Gas-Liquid chromatographic determination of cross-term second virial coefficients using glycerol. *Trans Faraday Soc.*, 1014–1031.
- David, W., Letcher, T. M., Ramjugernath, D., & Raal, J. D. (2003). Activity coefficients of hydrocarbon solutes at infinite dilution in the ionic liquid, 1-methyl-3-octyl-imidazolium chloride from gas-liquid chromatography. *Journal of Chemical Thermodynamics*, 35(8), 1335–1341.
- Domanska, U., Królikowska, M., Acree Jr, W. E., & Baker, G. A. (2011). Activity coefficients at infinite dilution measurements for organic solutes and water in the ionic liquid 1-ethyl-3-methylimidazolium tetracyanoborate. *The Journal of Chemical Thermodynamics*, 43(7),

1050–1057.

- Domańska, U., & Królikowski, M. (2012). Measurements of activity coefficients at infinite dilution for organic solutes and water in the ionic liquid 1-ethyl-3-methylimidazolium methanesulfonate. *Journal of Chemical Thermodynamics*, *54*, 20–27.
- Domańska, U., & Marciniak, A. (2008). Activity coefficients at infinite dilution measurements for organic solutes and water in the ionic liquid 1-butyl-3-methylimidazolium trifluoromethanesulfonate. *Journal of Physical Chemistry B*, *112*(35), 11100–11105.
- Domanska, U., Wlazło, M., & Karpinska, M. (2016). Activity coefficients at infinite dilution of organic solvents and water in 1-butyl-3-methylimidazolium dicyanamide. A literature review of hexane/hex-1-ene separation. *Fluid Phase Equilibria*, *417*, 50–61.
- Everett, D. H. (Dept. of P. C. of T. U. of B. (1965). Thermodynamics of adsorption from solution. *Trans Faraday Soc.*, (878), 878–899.
- Fedorov, M. V., & Kornyshev, A. A. (2014). Ionic liquids at electrified interfaces. *Chemical Reviews*, *114*(5), 2978–3036.
- Fosbøl, P. L., Pedersen, M. G., & Thomsen, K. (2011). Freezing point depressions of aqueous MEA, MDEA, and MEA-MDEA measured with a new apparatus. *Journal of Chemical and Engineering Data*, *56*(4), 995–1000.
- Francisco, M., Lago, S., Soto, A., & Arce, A. (2010). Essential oil deterpenation by solvent extraction using 1-ethyl-3-methylimidazolium 2-(2-methoxyethoxy) ethylsulfate ionic liquid. *Fluid Phase Equilibria*, *296*(2), 149–153.
- Ge, M. L., & Chen, J. B. (2011). Activity coefficients at infinite dilution of alkanes, alkenes, and alkyl benzenes in 1-ethyl-3-methylimidazolium diethylphosphate using gas-liquid chromatography. *Journal of Chemical and Engineering Data*, *56*(7), 3183–3187.
- Ge, M. L., Song, X. J., Li, G. M., Li, Y. H., Liu, F. Z., & Ma, H. L. (2012). Activity coefficients at infinite dilution of alkanes, alkenes, and alkyl benzenes in 1-butyl-3-methylimidazolium dibutylphosphate using gas-liquid chromatography. *Journal of Chemical and Engineering Data*, *57*(8), 2109–2113.
- Gibbard, H. F., & Fong, S. L. (1975). Freezing points and related properties of electrolyte solutions. III. The systems NaCl-CaCl<sub>2</sub>-H<sub>2</sub>O and NaCl-BaCl<sub>2</sub>-H<sub>2</sub>O. *Journal of Solution Chemistry*, *4*(10), 863–872.
- Grushka, E., & Grinberg, N. (2017). *Advances in chromatography Volume 53* (53rd ed.).
- Haghighi, H., Chapoy, A., & Tohidi, B. (2008). Freezing point depression of electrolyte solutions : experimental measurements and modeling using the cubic-plus-association equation of state. *Ind. Eng. Chem. Res.*, *47*, 3983–3989.
- Hall, D. L., Sterner, M. S., & Bodnar, R. J. (1988). Freezing point depression of NaCl-KCl-H<sub>2</sub>O solutions. *Economy Geology*, *83*, 197–202.
- Hayes, R., Warr, G. G., & Atkin, R. (2015). Structure and Nanostructure in Ionic Liquids. *Chemical Reviews*, *115*(13), 6357–6426.
- Hermanutz, F., Vocht, M. P., Panzier, N., & Buchmeiser, M. R. (2018). Processing of cellulose using ionic liquids. *Macromolecular Materials and Engineering*, 1–8.
- Huddleston, J. G., Willauer, H. D., Swatoski, R. P., Visser, A. E., & Rogers, R. D. (1998). Room temperature ionic liquids as novel media for “clean” liquid-liquid extraction. *Chemical Communications*, (16), 1765–1766.
- Hutchinson, J. M., & Kovacs, A. J. (1976). Simple phenomenological approach to the thermal behavior of glasses during uniform heating or cooling. *Journal of Polymer Science*, *14*(9), 1575–1590.

- Kato, R., & Gmehling, J. (2004). Activity coefficients at infinite dilution of various solutes in the ionic liquids methylsulfate, methoxyethylsulfate, dimethylphosphate, ethylpyridinium bis(trifluoromethylsulfonyl) imide and pyridiniummethoxyethylsulfate. *Fluid Phase Equilibria*, 226(1–2), 37–44.
- Kousksou, T., Jamil, A., Zeraoui, Y., & Dumas, J. P. (2007). Equilibrium liquidus temperatures of binary mixtures from differential scanning calorimetry. *Chemical Engineering Science*, 62(23), 6516–6523.
- Kovacs, A. J. (1966). Applicability of the free volume concept on relaxation phenomena in the glass transition range. *Rheologica Acta*, 5(4), 262–269.
- Królikowska, M., & Orawiec, M. (2016). Activity coefficients at infinite dilution of organic solutes and water in tributylethylphosphonium diethylphosphate using gas-liquid chromatography: thermodynamic properties of mixtures containing ionic liquids. *Journal of Chemical and Engineering Data*, 61(5), 1793–1802.
- Lago, S., Rodríguez, H., Arce, A., & Soto, A. (2014). Improved concentration of citrus essential oil by solvent extraction with acetate ionic liquids. *Fluid Phase Equilibria*, 361, 37–44.
- Lago, S., Rodríguez, H., Soto, A., & Arce, A. (2011). Deterpenation of citrus essential oil by liquid-liquid extraction with 1-alkyl-3-methylimidazolium bis(trifluoromethylsulfonyl)amide ionic liquids. *Journal of Chemical and Engineering Data*, 56(4), 1273–1281.
- Lei, Z., Chen, B., Koo, Y. M., & Macfarlane, D. R. (2017). Introduction: Ionic Liquids. *Chemical Reviews*, 117(10), 6633–6635.
- Liu, Y., Meyer, A. S., Nie, Y., Zhang, S., & Thomsen, K. (2018). Crystallization during cellulose spinning †. *Green Chemistry*, 20, 493–501.
- Liu, Y., Meyer, A. S., Nie, Y., Zhang, S., Zhao, Y., Fosbøl, P. L., & Thomsen, K. (2017). Freezing point determination of water – ionic liquid mixtures. *Journal of Chemical & Engineering Data*, 62, 2374–2383.
- MacFarlane, D. R., & Seddon, K. R. (2007). Ionic liquids-further progress on the fundamental issues. *Australian Journal of Chemistry*, 72(2), 3–10.
- Marekha, B. A., Bria, M., Moreau, M., & De Waele, I. (2015). Intermolecular interactions in mixtures of 1-n-butyl-3-methylimidazolium acetate and water: insights from IR, Raman, NMR spectroscopy and quantum chemistry calculations. *Journal of Molecular Liquids*, 210, 227–237.
- Martins, M. A. R., Coutinho, J. A. P., Pinho, S. P., & Domańska, U. (2015). Measurements of activity coefficients at infinite dilution of organic solutes and water on polar imidazolium-based ionic liquids. *Journal of Chemical Thermodynamics*, 91, 194–203.
- Martins, M. A. R., Domańska, U., Schröder, B., Coutinho, J. A. P., & Pinho, S. P. (2016). Selection of ionic liquids to be used as separation agents for terpenes and terpenoids. *ACS Sustainable Chemistry and Engineering*, 4(2), 548–556.
- Moïse, J. C., Mutelet, F., Jaubert, J. N., Grubbs, L. M., Acree, W. E., & Baker, G. A. (2011). Activity coefficients at infinite dilution of organic compounds in four new imidazolium-based ionic liquids. *Journal of Chemical and Engineering Data*, 56(7), 3106–3114.
- Moura Ramos, J. J., & Diogo, H. P. (2009). Are crystallization and melting the reverse transformation of each other? *Journal of Chemical Education*, 83(9), 1389.
- Noshadi, S., & Sadeghi, R. (2018). Differential scanning calorimetry determination of phase diagrams and water activities of aqueous carboxylic acid solutions. *Thermochimica Acta*, 663(March), 46–52.

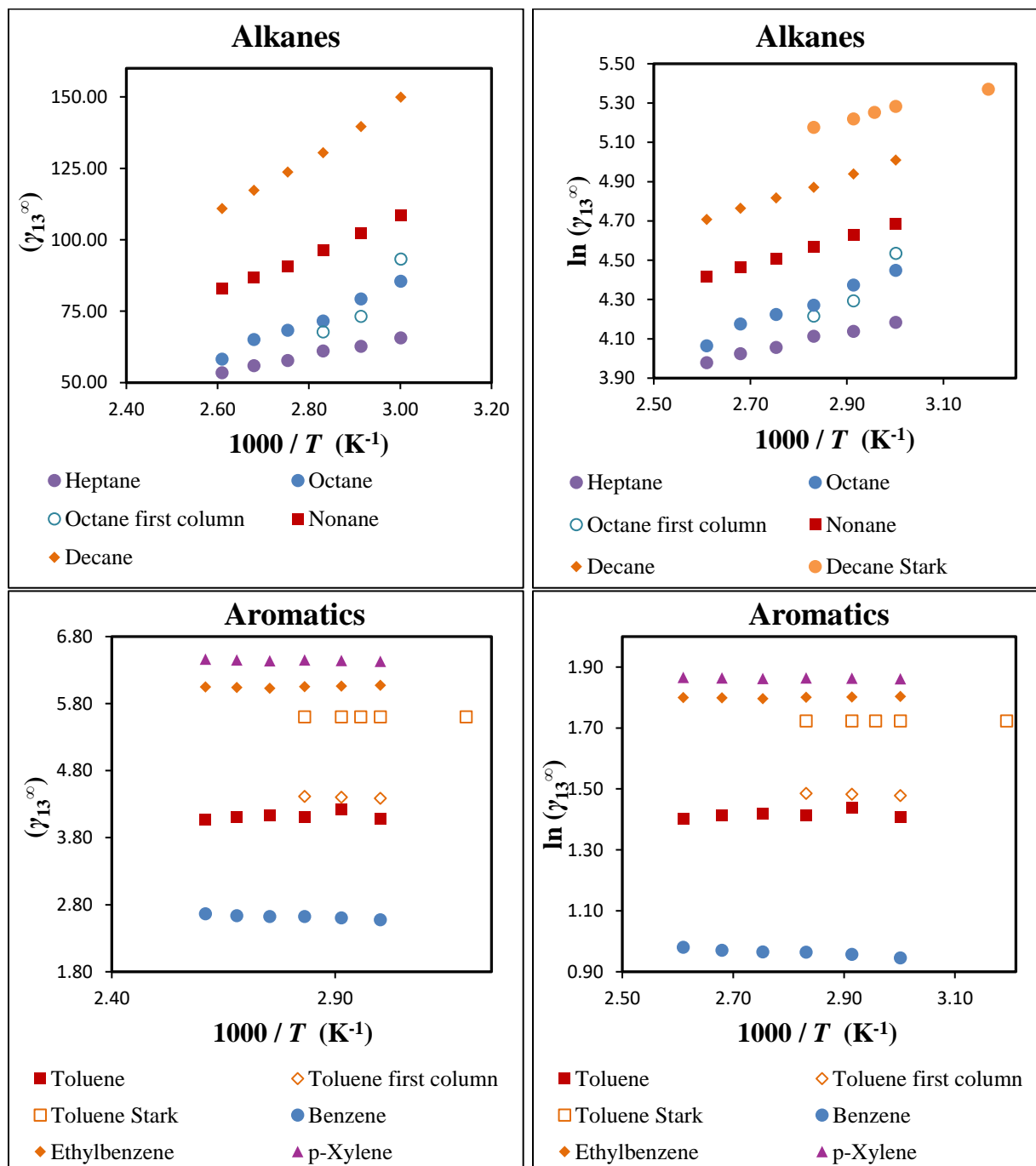
- Oakes, C. S., Bodnar, R. J., & Simonson, J. M. (1990). The system NaClCaCl<sub>2</sub>H<sub>2</sub>O: I. The ice liquidus at 1 atm total pressure. *Geochimica et Cosmochimica Acta*, 54(3), 603–610.
- Oliveira, C. M., Koshima, C. C., Capellini, M. C., Carvalho, F. H., Aracava, K. K., Gonçalves, C. B., & Rodrigues, C. E. C. (2013). Liquid-liquid equilibrium data for the system limonene+carvone+ethanol+water at 298.2K. *Fluid Phase Equilibria*, 360, 233–238.
- Pinho, S., & Macedo, E. (2004). Teaching electrolyte thermodynamics. *Chemical Engineering Education*, 38, 26–30.
- Poling, B. E., Prausnitz, J. M., & O’Connell, J. P. (2001). *The properties of gases and liquids* (5th ed.).
- Rasmussen, D. H., & MacKenzie, A. P. (1971). The glass transition in amorphous water. Application of the measurements to problems arising in cryobiology. *Journal of Physical Chemistry*, 75(7), 967–973.
- Rodbbush, W. H. (1918). The freezing points of concentrated solutions and the free energy of solution of salts. *Journal of the American Chemical Society*, 40(8), 1204–1213.
- Sandler, S. I. (1999). Chemical and engineering thermodynamics. In *John Wiley & Sons, New York*.
- Sell, C. S. (2003). *Fragrant Introduction to terpenoid chemistry*. Cambridge, UK: The Royal Society of Chemistry.
- Stark, A., Ondruschka, B., Zaitsau, D. H., & Verevkin, S. P. (2012). Biomass-derived platform chemicals: Thermodynamic studies on the extraction of 5-hydroxymethylfurfural from ionic liquids. *Journal of Chemical and Engineering Data*, 57(11), 2985–2991.
- Vekariya, R. L. (2017). A review of ionic liquids : applications towards catalytic organic transformations. *Journal of Molecular Liquids*, 227, 44–60.
- Wasserscheid, P., & Welton, T. (2002). *Ionic Liquids in Synthesis* (Vol. 8).
- Weng, L., Li, W., & Zuo, J. (2011). DSC determination of partial ternary phase diagrams of methanol/sodium chloride/water and propylene glycol/sodium chloride/water and their applications for synthesized diagrams. *Thermochimica Acta*, 512(1–2), 225–232.
- Wilkes, J. S. (2004). Properties of ionic liquid solvents for catalysis. *Journal of Molecular Catalysis A: Chemical*, 214(1), 11–17.
- Wlazło, M., Gawkowska, J., & Domańska, U. (2016). Separation based on limiting activity coefficients of various solutes in 1-allyl-3-methylimidazolium dicyanamide ionic liquid. *Industrial and Engineering Chemistry Research*, 55(17), 5054–5062.
- Zafarani-Moattar, M. T., & Majdan-Cegincara, R. (2007). Viscosity, density, speed of sound, and refractive index of binary mixtures of organic solvent + Ionic liquid, 1-Butyl-3-methylimidazolium hexafluorophosphate at 298.15 K. *Journal of Chemical and Engineering Data*, 52(6), 2359–2364.

## Appendix A.

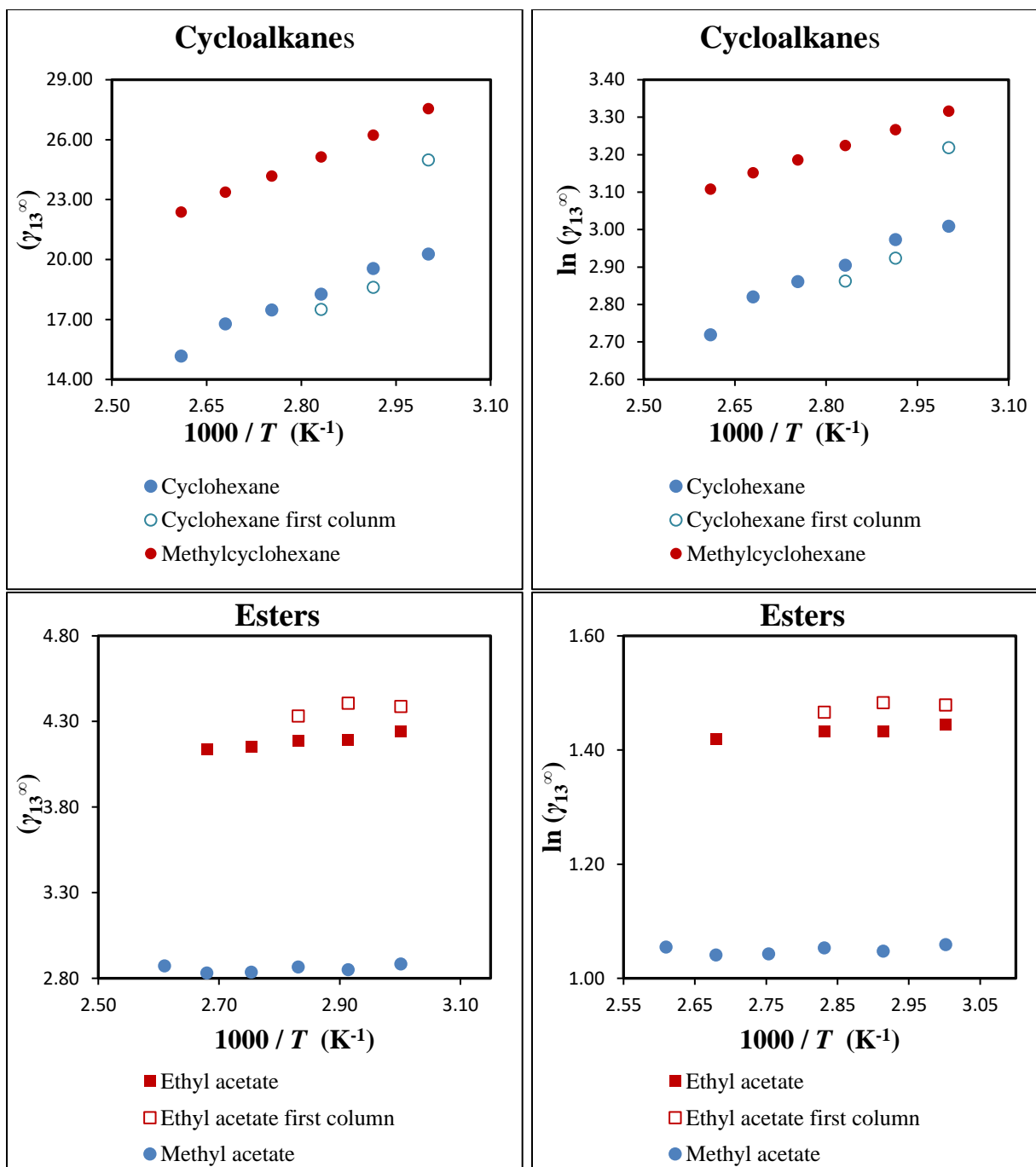
**Table A 1.** Values of  $\gamma_{13}^{\infty}$  for all solutes.

| Organic solutes         | [C <sub>4</sub> min][Oac] |        |        |        |        |        |
|-------------------------|---------------------------|--------|--------|--------|--------|--------|
| <i>T/K</i>              | 333.15                    | 343.15 | 353.15 | 363.15 | 373.15 | 383.15 |
| Heptane                 | 65.68                     | 62.75  | 61.12  | 57.80  | 55.96  | 53.47  |
| Octane                  | 85.54                     | 79.37  | 71.61  | 68.35  | 65.10  | 58.27  |
| Nonane                  | 108.56                    | 102.38 | 96.27  | 90.83  | 86.71  | 82.85  |
| Decane                  | 149.94                    | 139.66 | 130.48 | 123.73 | 117.34 | 110.92 |
| Cyclohexane             | 20.27                     | 19.56  | 18.27  | 17.48  | 16.79  | 15.16  |
| Methylcyclohexane       | 27.55                     | 26.23  | 25.13  | 24.18  | 23.38  | 22.38  |
| Benzene                 | 2.57                      | 2.60   | 2.62   | 2.62   | 2.64   | 2.67   |
| Ethylbenzene            | 6.07                      | 6.06   | 6.05   | 6.03   | 6.04   | 6.05   |
| Toluene                 | 4.09                      | 4.22   | 4.11   | 4.13   | 4.11   | 4.07   |
| p-Xylene                | 6.43                      | 6.44   | 6.45   | 6.44   | 6.45   | 6.46   |
| Methyl acetate          | 2.88                      | 2.85   | 2.87   | 2.84   | 2.83   | 2.87   |
| Ethyl acetate           | 4.24                      | 4.19   | 4.19   | 4.15   | 4.14   | ----   |
| THF                     | 3.04                      | 2.91   | 2.89   | 2.86   | 2.84   | 2.86   |
| 1,4-dioxane             | 2.25                      | 2.28   | 2.28   | 2.28   | 2.26   | 2.16   |
| Diethyl ether           | 10.12                     | 9.91   | 9.86   | 9.67   | 9.58   | 9.66   |
| Acetonitrile            | 0.91                      | 0.95   | 0.94   | 0.95   | 0.94   | 0.96   |
| Pyridine                | 1.26                      | 1.27   | 1.29   | 1.29   | ----   | 1.31   |
| Thiophene               | 1.23                      | 1.29   | 1.33   | 1.36   | 1.40   | 1.45   |
| Acetone                 | 2.07                      | 2.04   | 2.08   | 2.05   | 2.03   | 1.91   |
| 2-Butanone              | 2.25                      | 2.27   | 2.29   | 2.27   | 2.26   | 2.28   |
| T/K                     | 383.15                    | 393.15 | 403.15 |        |        |        |
| Methanol                | ----                      | ----   | ----   | 0.04   | 0.05   | 0.05   |
| Ethanol                 | ----                      | ----   | ----   | 0.08   | 0.08   | 0.09   |
| 1-Propanol              | ----                      | ----   | ----   | 0.10   | 0.12   | 0.13   |
| 2-Propanol              | ----                      | ----   | ----   | 0.12   | 0.14   | 0.15   |
| Isobutanol              | ----                      | ----   | ----   | 0.12   | 0.14   | 0.15   |
| 1-Butanol               | ----                      | ----   | ----   | 0.12   | 0.14   | 0.16   |
| 2-Butanol               | ----                      | ----   | ----   | 0.15   | 0.18   | 0.19   |
| Tert-butanol            | ----                      | ----   | ----   | 0.23   | 0.28   | 0.31   |
| T/K                     | 353.15                    | 363.15 | 373.15 | 383.15 | 393.15 | 403.15 |
| $\alpha$ - pinene       | 33.69                     | 33.41  | 32.29  | 26.68  | 25.26  | 25.90  |
| $\beta$ - pinene        | 25.37                     | 24.42  | 24.20  | 20.59  | 19.68  | 20.00  |
| Limonene                | 23.12                     | 23.19  | 23.41  | 24.77  | 25.09  | 24.18  |
| p - cymene              | 15.09                     | 15.42  | 16.11  | 16.49  | ----   | 19.45  |
| $\alpha$ - pinene oxide | 9.37                      | 9.55   | 9.77   | 10.21  | 10.47  | 10.62  |
| Menthone                | 11.56                     | 11.26  | 11.10  | 8.90   | 8.61   | 9.15   |

|            |       |       |       |       |       |       |
|------------|-------|-------|-------|-------|-------|-------|
| Eucalyptol | 20.71 | 20.37 | 19.94 | 15.21 | 14.64 | 15.68 |
| Fenchone   | 9.00  | 8.80  | 8.66  | 8.52  | 8.45  | 8.15  |
| Linalool   | ----  | ----  | ----  | 3.72  | ----  | 7.49  |
| Geraniol   | ----  | ----  | ----  | ----  | 0.18  | 0.37  |

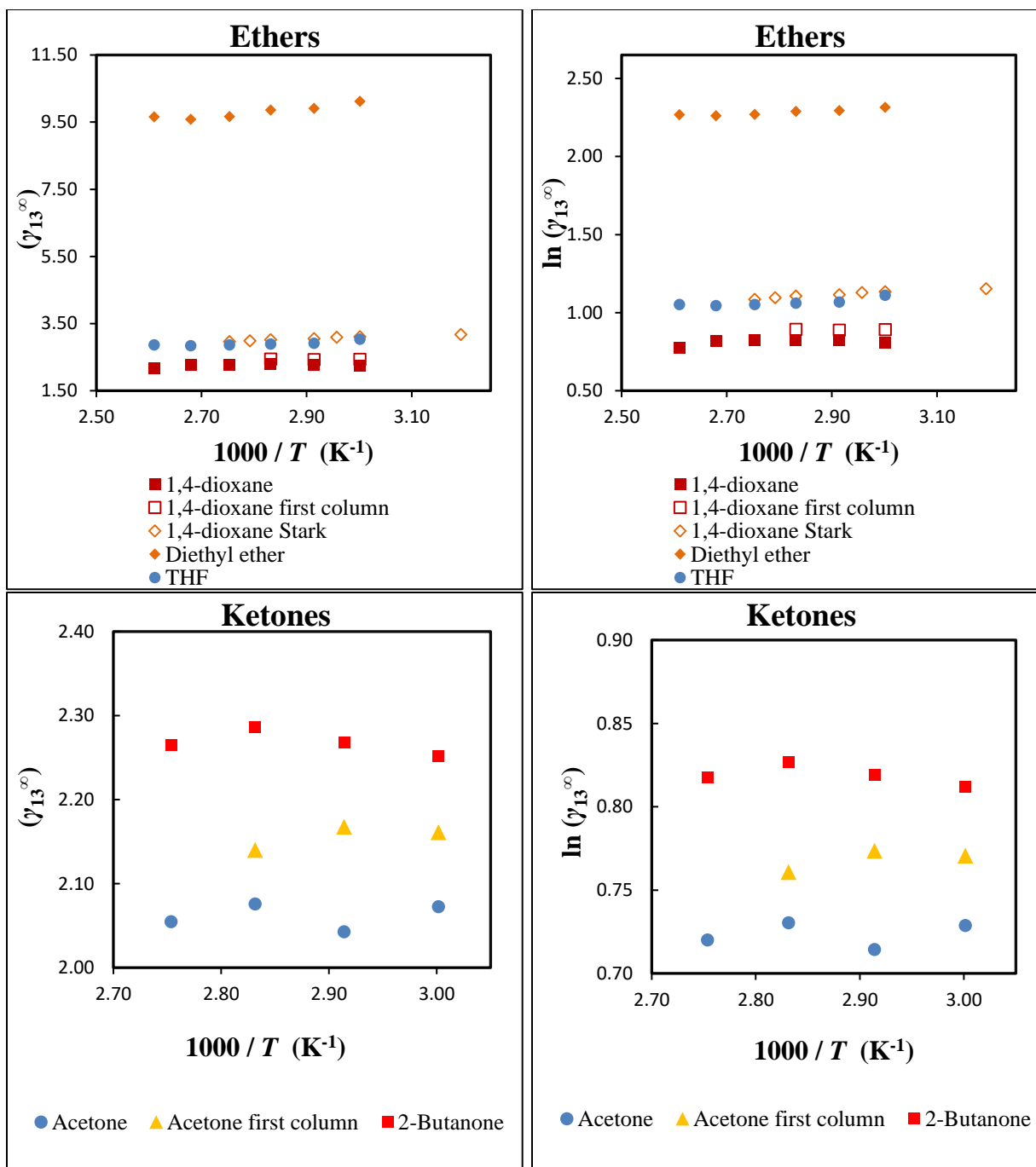


**Figure A. 1.** Values of activity coefficient at infinity dilution of families: alkanes and aromatics

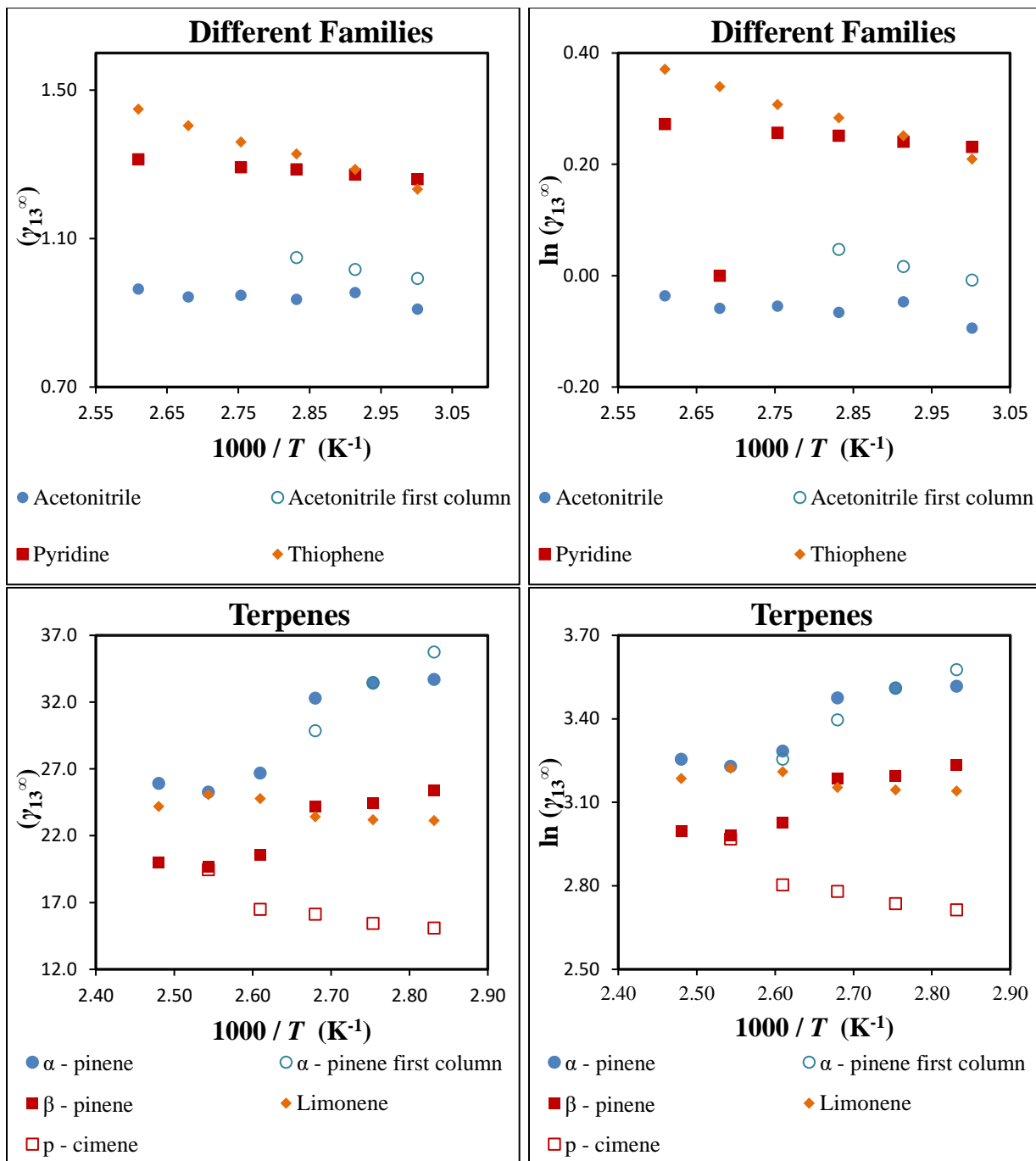


**Figure A. 2.** Values of activity coefficient at infinity dilution of families: cycloalkanes and esters

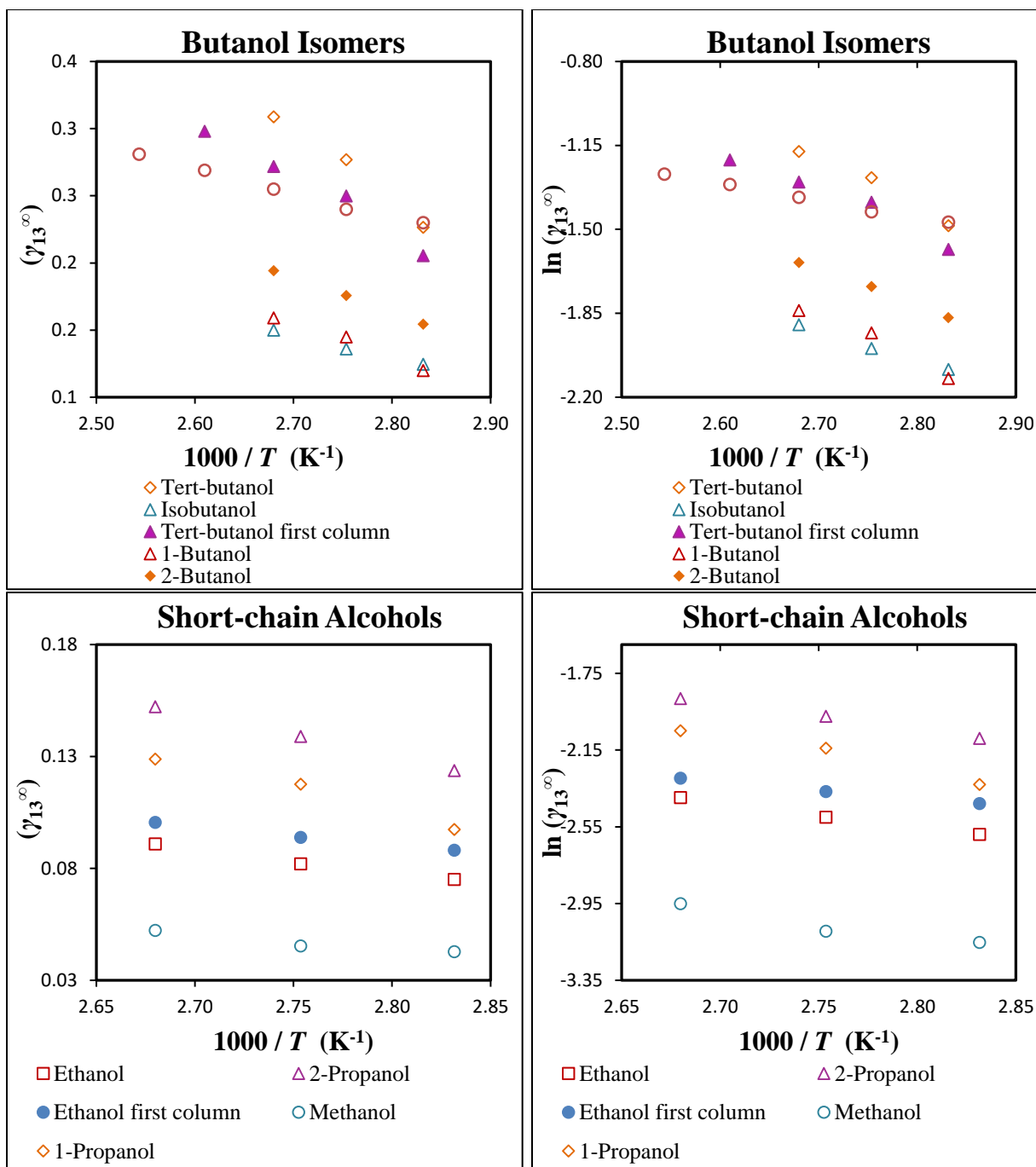




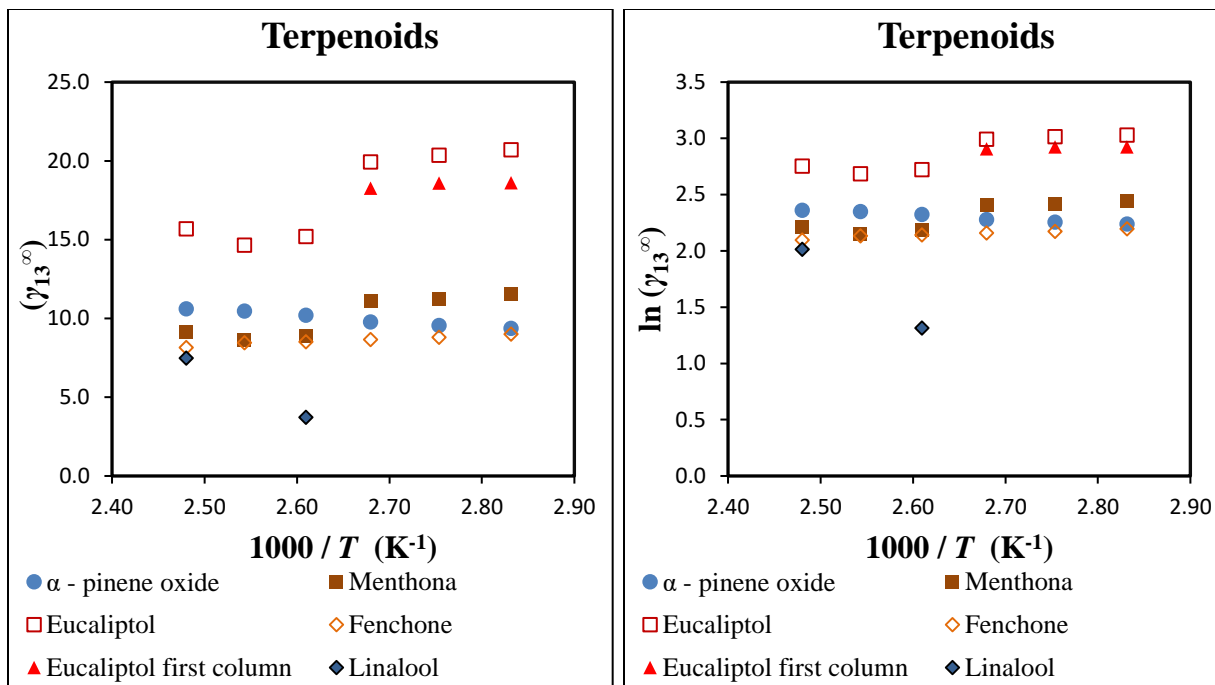
**Figure A. 3.** Values of activity coefficient at infinity dilution of families: ethers and ketones



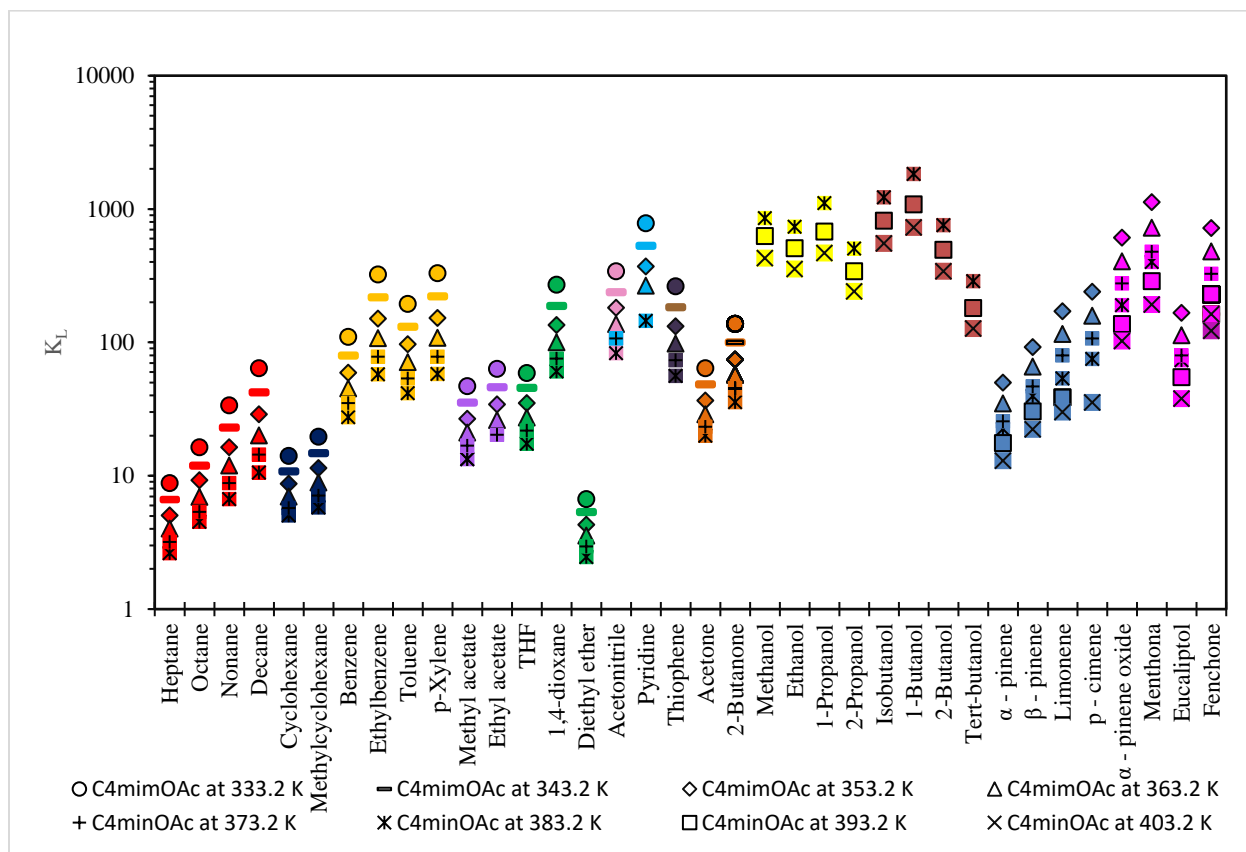
**Figure A. 4.** Values of activity coefficient at infinity dilution of families: different families and terpenes



**Figure A. 5.** Values of activity coefficient at infinity dilution of families: butanol isomers and short-chain alcohols

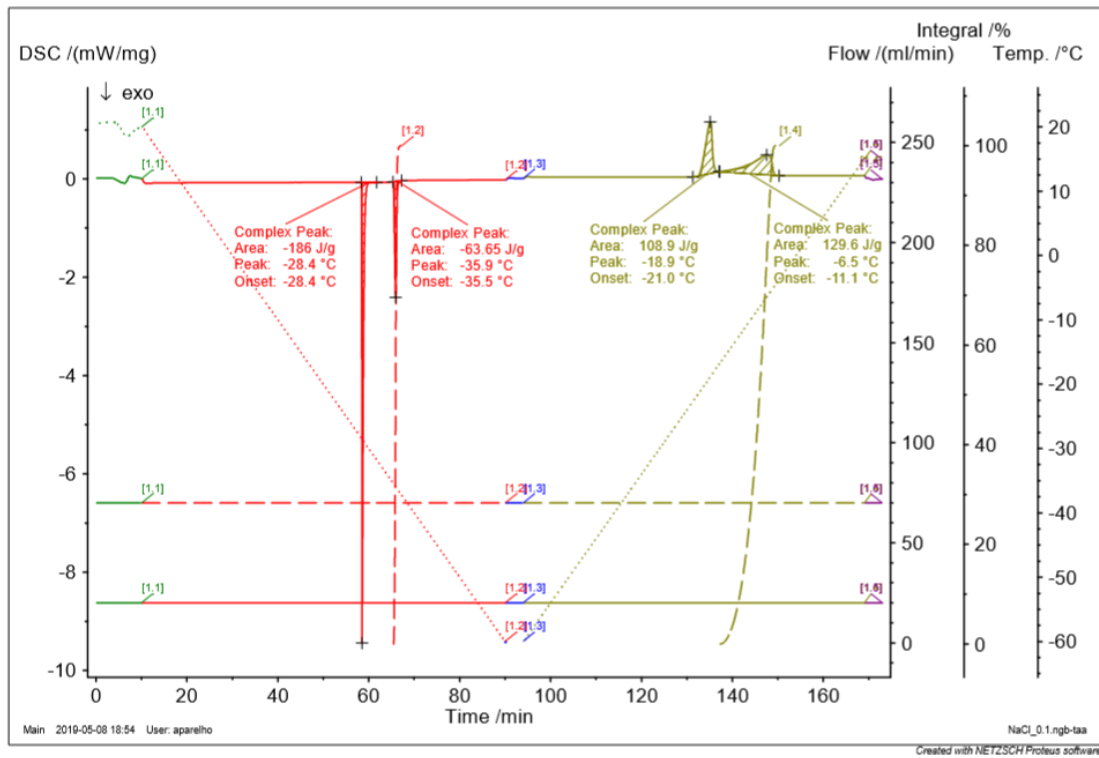


**Figure A. 6.** Values of activity coefficient at infinity dilution of families of terpenoids

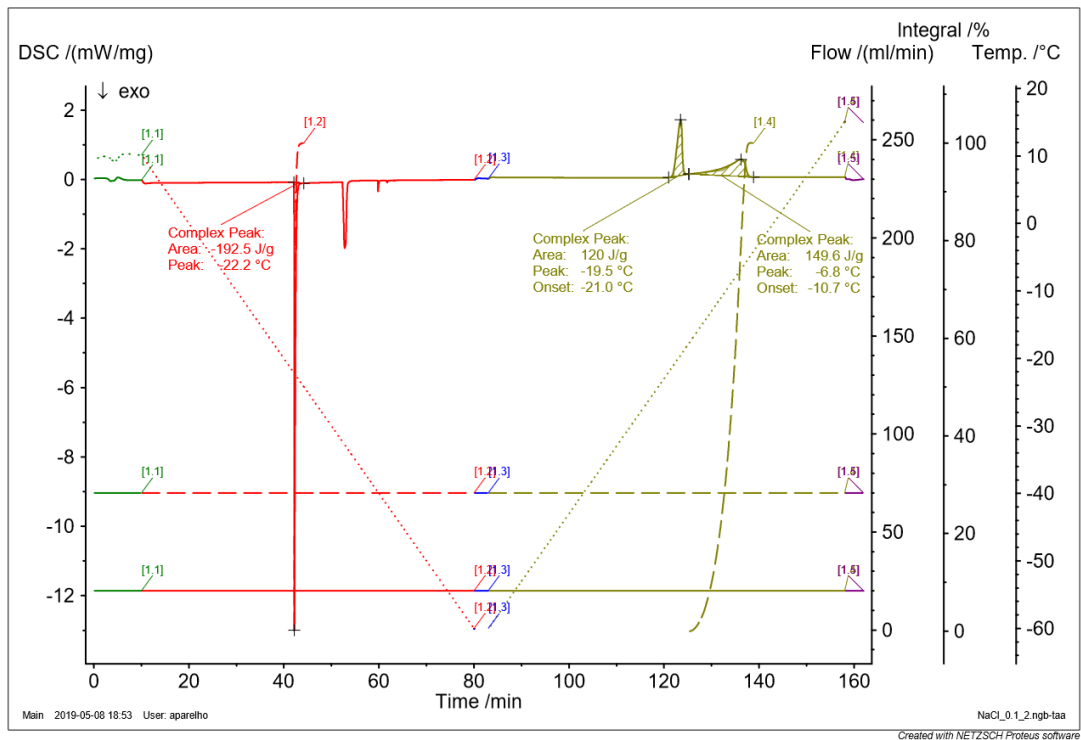


**Figure A. 7.** Experimental (gas + liquid) partition coefficients,  $K_L$ , for organic solutes

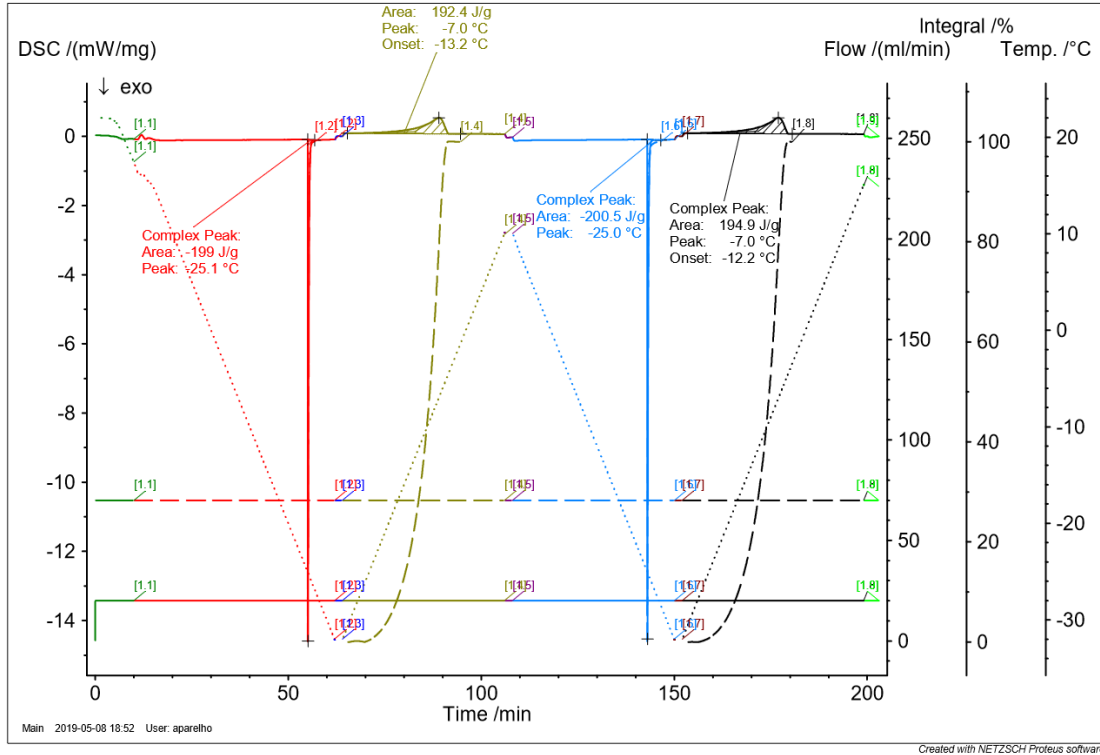
# Appendix B.



**Figure B. 1.** Differential scanning calorimetry of first analysis of NaCl aqueous solution



**Figure B. 2.** Differential scanning calorimetry of second analysis of NaCl aqueous solution



**Figure B. 3.** Differential scanning calorimetry of third analysis of NaCl aqueous solution